JGP Journal of General Physiology

ARTICLE

Angiotensin 1–7 prevents the excessive force loss resulting from 14- and 28-day denervation in mouse EDL and soleus muscle

Hind Albadrani[1,2], T. Ammar[1], Michael Bader[3,4,5,6], and Jean-Marc Renaud[1]

Denervation leads to muscle atrophy, which is described as muscle mass and force loss, the latter exceeding expectation from mass loss. The objective of this study was to determine the efficiency of angiotensin (Ang) 1–7 at reducing muscle atrophy in mouse extensor digitorum longus (EDL) and soleus following 14- and 28-d denervation periods. Some denervated mice were treated with Ang 1–7 or diminazene aceturate (DIZE), an ACE2 activator, to increase Ang 1–7 levels. Ang 1–7/DIZE treatment had little effect on muscle mass loss and fiber cross-sectional area reduction. Ang 1–7 and DIZE fully prevented the loss of tetanic force normalized to cross-sectional area and accentuated the increase in twitch force in denervated muscle. However, they did not prevent the shift of the force–frequency relationship toward lower stimulation frequencies. The Ang 1–7/DIZE effects on twitch and tetanic force were completely blocked by A779, a MasR antagonist, and were not observed in MasR$^{-/-}$ muscles. Ang 1–7 reduced the extent of membrane depolarization, fully prevented the loss of membrane excitability, and maintained the action potential overshoot in denervated muscles. Ang 1–7 had no effect on the changes in α-actin, myosin, or MuRF-1, atrogin-1 protein content or the content of total or phosphorylated Akt, S6, and 4EPB. This is the first study that provides evidence that Ang 1–7 maintains normal muscle function in terms of maximum force and membrane excitability during 14- and 28-d periods after denervation.

Introduction

Muscle atrophy is defined as a decrease in muscle mass that eventually leads to partial or complete muscle wasting. Muscle atrophy occurs in a variety of conditions, including chronic diseases such as heart or kidney failure and limb immobilization, and following a complete loss of muscle activity after spinal cord injury or peripheral nerve injury (Martinez et al., 2010; Xu et al., 2012; MacDonald et al., 2014). Muscle atrophy has two major consequences. First, there is a decrease in force associated with loss of muscle mass and contractile components, which deteriorates quality of life as patients become unable to perform certain tasks, such as walking or moving, or increases the risk of accidents while performing those tasks. Second, skeletal muscle plays major metabolic roles, such as glucose homeostasis, and these roles are then diminished or lost with the loss of muscle mass.

Atrophy associated with denervation involves significant muscle mass loss, reaching 50% within just 14 d, resulting in smaller fiber cross-sectional area (CSA; Pellegrino and Franzini, 1963). More importantly, there is a net loss of CSA normalized maximum tetanic force by 30–40% in <10 d (Finol et al., 1981). A net loss of normalized tetanic force implies that force loss exceeds expectation from mass loss. At least two mechanisms are involved in this force loss. First, the cell membrane depolarizes from a mean of approximately −75 mV to −60/−55 mV in 4 d due to greater Na^+ permeability and lower K^+ permeability (Albuquerque and Thesleff, 1968; Albuquerque et al., 1971; Vyskocil et al., 1973; Kotsias and Venosa, 1987). Na^+ channels become inactivated when the cell membrane depolarizes, which then reduces membrane excitability. That is, smaller action potential amplitudes are generated by some fibers while other fibers fail to generate action potentials; failure to generate action potential occurs when the resting membrane potential (E_M) becomes less than −60 mV (Cairns et al., 1997; Ammar et al., 2015). As a consequence of lower membrane excitability, less Ca^{2+} is released by sarcoplasmic reticulum and less force is generated. Second, degeneration of myofibrils starts at the fiber periphery and is quite significant by 14 d; after 28 d, myofibril number and diameters are significantly reduced, resulting in

[1]University of Ottawa, Department of Cellular and Molecular Medicine, Ottawa, Ontario, Canada; [2]Majmaah University, Department of Medical Laboratory Sciences, Al Majma'ah, Saudi Arabia; [3]Max-Delbrück Center for Molecular Medicine, Berlin-Buch, Germany; [4]University of Lübeck, Institute for Biology, Lübeck, Germany; [5]Charité University Medicine, Berlin, Germany; [6]German Center for Cardiovascular Research, Berlin, Germany.

Correspondence to Jean-Marc Renaud: jmrenaud@uottawa.ca.

fiber areas completely devoid of contractile machinery (Pellegrino and Franzini, 1963).

Several studies have attempted to attenuate or fully prevent the atrophy process following denervation. Some of these studies include chronic stimulations (e.g., 9 h/d every 15 s to 2 h for 15–104 d), IGF-1 analogues or β-adrenergic agonists to activate the Akt/mTOR hypertrophic signaling pathway (Al-Amood et al., 1986; Zeman et al., 1987; Vandenburgh et al., 1991; Hinkle et al., 2002; Shavlakadze et al., 2005), and phosphodiesterase 4 inhibition to increase cAMP levels (Hinkle et al., 2005). All these studies reported significant reductions in the loss of muscle mass, protein content, force, and fiber CSA; however, none of these approaches allowed for a full prevention of muscle atrophy (i.e., keep all values close to those of normal innervated muscles). Finally, an inhibition of ActRIIB, the myostatin receptor that inhibits muscle growth, completely fails to prevent the atrophy process in denervated muscles (MacDonald et al., 2014).

Angiotensin (Ang) 1–7 is the main peptide of the nonclassical renin-angiotensin system (Santos et al., 2018). It is produced by angiotensin-converting enzyme 2 (ACE2), which removes one amino acid from Ang II. Ang 1–7 acts as a local vasodilator counteracting the vasoconstriction effect of Ang II (Fu et al., 2014; de Moraes et al., 2017). ACE2 is also expressed in the sarcolemma of skeletal muscle fibers (Fernandes et al., 2010; Riquelme et al., 2014), along with the Ang II receptor, AT-1, and the Ang 1–7 G protein–coupled transmembrane receptor MasR (Cisternas et al., 2015; Morales et al., 2015a). More importantly, Ang II activates the MuRF-1 and atrogin-1 atrophic pathway, resulting in greater myonuclear apoptosis, smaller fiber CSA, tetanic force, and myosin expression, while Ang 1–7 not only activates the Akt–mTOR hypertrophic pathway but also inhibits Ang II– and transforming growth factor β (TGF-β)–induced activation of the atrophic pathway (Cisternas et al., 2015; Meneses et al., 2015; Ábrigo et al., 2016).

Activation of the MasR–Ang1-7 pathway improves the skeletal muscle metabolic profile associated with a high-fat diet and insulin resistance, and it reverses the atrophy associated with muscle immobilization, muscular dystrophy, sepsis, cancer, Ang II, and TGF-β (Marcus et al., 2013; Acuña et al., 2014; Echeverría-Rodríguez et al., 2014; Morales et al., 2015b; Ábrigo et al., 2016; Morales et al., 2016; Murphy et al., 2019). It remains to be determined how effective Ang 1–7 is at preventing muscle atrophy and function loss following denervation. The objective of this study was to determine the effectiveness of Ang 1–7 in preventing the decrease in muscle mass, fiber CSA, and force loss that occurs after 14- and 28-d denervation periods. For this, the left leg was denervated and mice treated with Ang 1–7 using an osmotic pump or diminazene aceturate (DIZE), an ACE2 activator, by gavage. At a dose of 350–390 ng/kg/min, plasma and kidney Ang 1–7 levels increase by approximately twofold (Oh et al., 2012; Mori et al., 2014). However, at a lower dose of 100 ng/kg/d, Ang 1–7 significantly reduced skeletal muscle atrophy and apoptosis induced by endotoxin, Ang II, TGF-β, or disuse (Cisternas et al., 2015; Meneses et al., 2015; Morales et al., 2015b; Ábrigo et al., 2016; Morales et al., 2016) while it restores muscle strength in dystrophic mice (Acuña et al., 2014). So, for this study, the lower Ang 1–7 dose was used. At a dose of 15 mg/kg/d, as used in this study, DIZE increases plasma Ang 1–7 levels by almost fourfold (Zhang et al., 2015). The results of this study show that Ang 1–7 is not effective at reducing muscle mass loss and fiber CSA reduction but is fully effective at preventing maximum tetanic force loss, because Ang 1–7 reduces the extent of the membrane depolarization that occurs during denervation, allowing for full preservation of membrane excitability and action potential overshoot.

Materials and methods

Animals

Wild-type CD-1 mice and Mas receptor–knockout mice ($MasR^{-/-}$) generated by Walther et al. (1998) were used. Mice were bred, fed ad libitum, and housed according to the guidelines of the Canadian Council for Animal Care. The Animal Care Committee of the University of Ottawa approved all surgical and experimental procedures.

Genotyping

All $MasR^{-/-}$ mice were genotyped using NucleoSpin Tissue kit (catalog no. 740952.250; Macherey Nagel). Briefly, a 2–3-mm piece of ear was incubated in a proteinase digestion buffer overnight at 56°C. After adding elution buffer, digested tissues were incubated sample at 70°C for 10 min before being centrifuged 5 min at 11,000 *g*. Supernatant was washed with ethanol, and the extracted DNA was subjected to PCR using the following primers: forward, 5′-GCCGTTGCCCTCCTGGCGCCTGGG-3′; reverse, 5′-GGCAGCGCGGCTATCGTGG-3′. Bands were visualized using gel Doc imager (Bio-Rad).

Denervation procedure: Ang 1–7, DIZE, and A779 treatment

Mice received a subcutaneous injection of buprenorphine (0.05 mg/kg) before surgery. For the surgery, mice were anesthetized using 2.5–3.5% isoflurane, and 1 ml sterile 0.9% NaCl solution was injected in the neck to minimize dehydration. A small posterolateral (mid-thigh) incision was made where 3–4 mm of the sciatic nerve sciatic was cut and removed. For Ang 1–7 treatment (MilliporeSigma, Canada) with and without A779 (Tocris Bioscience), a small incision was made in the subscapular area to create a pocket to insert an osmotic pump (Durect Co. 1002 and 1004 model; Alzet) just under the skin. Both Ang 1–7 and A779 were administered at dose of 100 ng/kg/min for the entire denervation period of either 14 or 28 d. A topical application of 2% bupivacaine was placed on the wound. DIZE (Santa Cruz Biotechnology), on the other hand, was administered by oral gavage at a dosage of 15 mg/kg/d without or with treatment with A779 by osmotic pump as described above. One group of denervated mice received sucrose at 1 g/kg/d also by oral gavage as a control for DIZE treatment.

Force measurement

Prior to muscle excision, mice were anaesthetized with a single intraperitoneal injection of 65 mg ketamine/13 mg xylazine/2 mg acepromazine per kilogram body weight and sacrificed by cervical dislocation. Extensor digitorum longus (EDL) and soleus were then dissected out for in vitro experiments. Muscles were

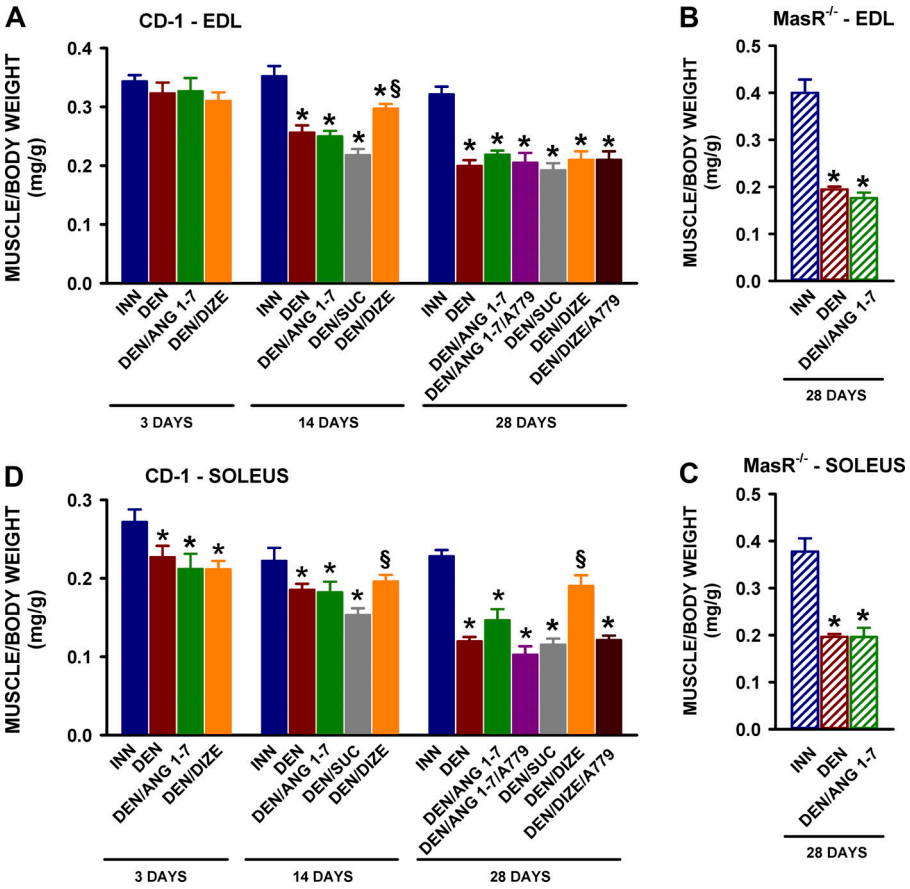

Figure 1. **Ang 1–7/DIZE significantly reduced muscle weight loss at 14-d denervation for EDL and at 14- and 28-d denervation for soleus; an effect not observed in the presence of A779 or in MasR$^{-/-}$ soleus.** Muscle weight expressed as a ratio of body weight of (A) wild type (CD-1) and (B) MasR$^{-/-}$ EDL, (C) wild type and (D) MasR$^{-/-}$ soleus. Ang 1–7 and A779 were delivered using an osmotic pump (100 ng/kg/min), while sucrose (1 g/kg/d) and DIZE (15 mg/kg/d) were given once daily by gavage. INN, innervated; DEN, denervated; SUC, sucrose. Vertical bars represent SE of 5–19 muscles. *, mean muscle weight significantly different from that of innervated muscles; §, mean muscle weight significantly different from that of denervated or denervated/sucrose muscles (ANOVA and LSD, $P < 0.05$).

positioned horizontally in a Plexiglas chamber. One end of the muscle was fixed to a stationary hook, while the other end was attached to a force transducer (model no. 400A; Aurora Scientific Canada). The transducer was connected to a KCPI3104 data acquisition system (Keithley), and data were recorded at 5 kHz.

Muscle length was adjusted to give maximal tetanic force while muscles were stimulated every 100 s. The force–frequency relationship was measured after a 30-min equilibrium period. Frequency 50 represented the stimulation frequency at which muscles generated 50% of maximum force (i.e., tetanic force). The force–frequency relationship of each muscle was fitted by nonlinear regression analysis to a sigmoidal curve (version 13; SigmaPlot) from which frequency 50 was calculated as follows:

$$FORCE = \frac{FORmax}{1 + e^{\left[\frac{-(Freq-FF50)}{C}\right]}},$$

where FORCE is the measured force in newtons per square centimeter (N/cm^2), FF50 is frequency 50, FORmax is the maximum tetanic force, Freq is the stimulation frequency, and C is a constant.

Twitch and tetanic force, defined as the force developed following a single stimulation pulse or a train of pulses, respectively, was calculated as the difference between the maximum force during a contraction and the force measured 5 ms before the contraction was elicited. Forces are presented in N and N/cm^2 (i.e., normalized to CSA). At the end of each experiment, muscle weight (free of tendons) was measured and converted to a volume using a density of 1.06 g/cm^3, and CSA was calculated by dividing muscle volume by the length measured in the bath. Time to peak was defined as the time interval between the first stimulation and the time force reached its maximum during a contraction. Half-relaxation time for a twitch contraction was defined as the time interval between the time at which force reached a peak and the time force had decayed by 50% during the relaxation phase, while for a tetanic contraction, it was the time interval between the time the last stimulation was applied and the time when force had decayed by 50% during the relaxation phase.

Stimulation

Electrical stimulations were applied across two platinum wires (4 mm apart) located on opposite sides of the muscles. They were connected to a Grass S88X stimulator and a Grass stimulation isolation unit (Grass Technologies/Astro-Med). Twitch contractions were elicited with a 0.3-ms, 10-V (supramaximal voltage) pulse, while tetanic contractions were elicited with 400-ms trains of the same pulses at frequencies varying between 10 and 200 Hz.

Physiological solutions

Physiological saline solution contained (in mM) 118.5 NaCl, 4.7 KCl, 2.4 $CaCl_2$, 3.1 $MgCl_2$, 25 $NaHCO_3$, 2 NaH_2PO_4, and 5.5 D-glucose. Solutions were continuously bubbled with 95% O_2–5% CO_2 to maintain a pH of 7.4. Experimental temperature

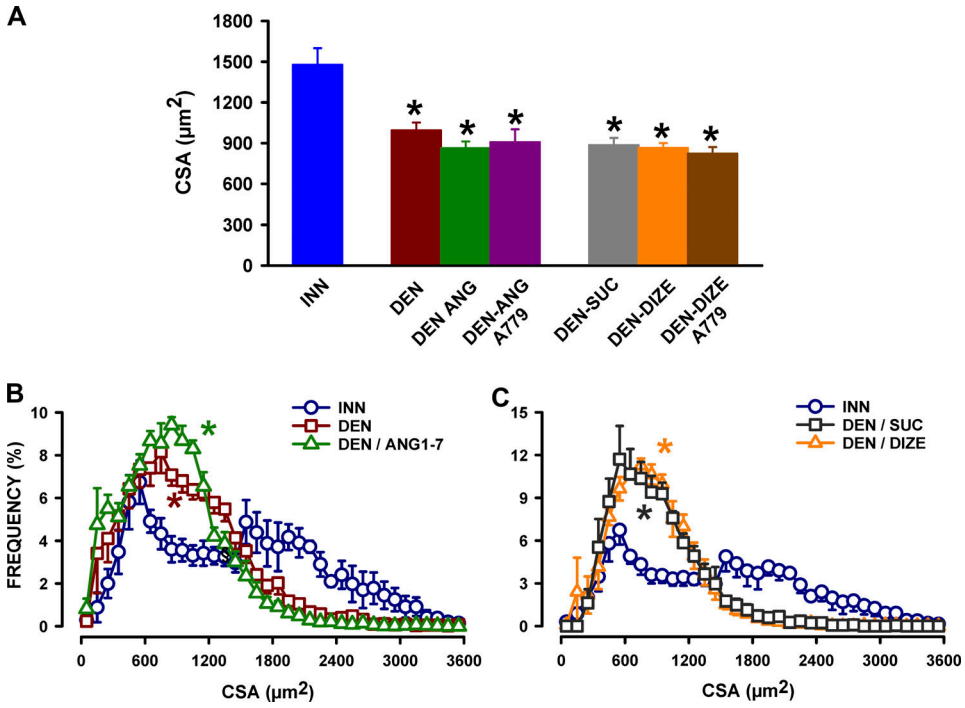

Figure 2. **Ang 1–7 did not prevent the decrease in fiber CSA associated with 28-d denervation in EDL.** (A) Mean fiber CSA values; fiber CSA distribution of (B) innervated, denervated EDL without or with Ang 1–7 treatment; (C) innervated, sucrose-treated, and DIZE-treated denervated EDL. CSA values were divided in bin of 100 μm^2, and the number of fibers in each bin is presented as a percentage of the total number of fibers analyzed. For clarity, the CSA distributions of EDL from mice treated with the MasR antagonist, A779, is not shown, as it was similar to that of denervated/Ang 1–7 and denervated/DIZE. The CSA frequency distribution was first determined for each muscle, and then mean and SE (vertical bars) were calculated from four or five muscles (with a total number of fibers ranging between 2,728 and 4,797). *, CSA distribution was significantly shifted toward lower CSA when compared with innervated (ANOVA, and LSD, $P < 0.05$).

was 37°C. Total flow of solutions in the muscle chamber was 15 ml/min, being split just above and below the muscle in order to prevent any buildup of reactive oxygen species, which is quite large at 37°C and deleterious in terms of force generation (Edwards et al., 2007).

Resting E_M and action potential measurements

Once force measurements were completed as described above, resting E_M and action potential were measured by penetrating individual fibers located at the surface of both EDL and soleus muscles with glass microelectrodes as previously described (Ammar et al., 2015). Briefly, microelectrode tip resistances were 7–10 MΩ and that of the reference electrode ∼1 MΩ. All electrodes were filled with 3 M KCl. A recording was rejected when the change in potential upon penetration was not a sharp drop or when the microelectrode potential did not return to zero upon withdrawal from the fiber. Stimulating electrodes for force measurements were disconnected. Instead, single action potentials were elicited using fine platinum wires 2 mm apart placed as close as possible to the surface fibers and moved laterally to stimulate fibers in the region where the microelectrode was positioned. This approach was used to reduce the extent of contracting fibers and prevent the breaking or dislodging of microelectrodes. To further reduce the number of contracting fibers, action potentials were triggered using a single 2- to 10-V, 0.3-ms square stimulating pulse; usually, a low voltage was enough to trigger an action potential in innervated muscle fibers, while higher voltages were often necessary with denervated fibers. When an action potential was not triggered, voltage was always increased to 10 V to properly verify that the fiber was unexcitable. Data were digitized using a KCP13104 data acquisition system (Keithley) at 400 kHz.

The number of excitable fibers, resting E_M, action potential, and the overshoot maximum rate of depolarization were determined in 5–15 fibers in each muscle. Overshoot was taken from the action potential peak, while maximum rate of depolarization was first calculated by linear regression analysis of every 10 data points and taken from the peak value. Individual fiber values for each muscle were averaged, and the final mean was calculated from the muscle average values. For these parameters, the number of samples are reported as number of tested fibers/number of muscles used.

Fiber typing and CSA

EDL and soleus muscles were embedded in Tissue-Tek at a length similar to that in situ, frozen in isopentane precooled in liquid nitrogen, and stored at −80°C. 10-μm sections were cut at −20°C using a cryostat (Leica CM 1850), placed on positive-charged glass slides, and stored at −80°C. Sections were stained using a Mouse on Mouse (MOM) fluorescein kit (catalog no. FMK-2201; MJS Biolynx) for type I, IIA, and IIB fibers. Briefly, a section was incubated for 1 h in MOM mouse Ig

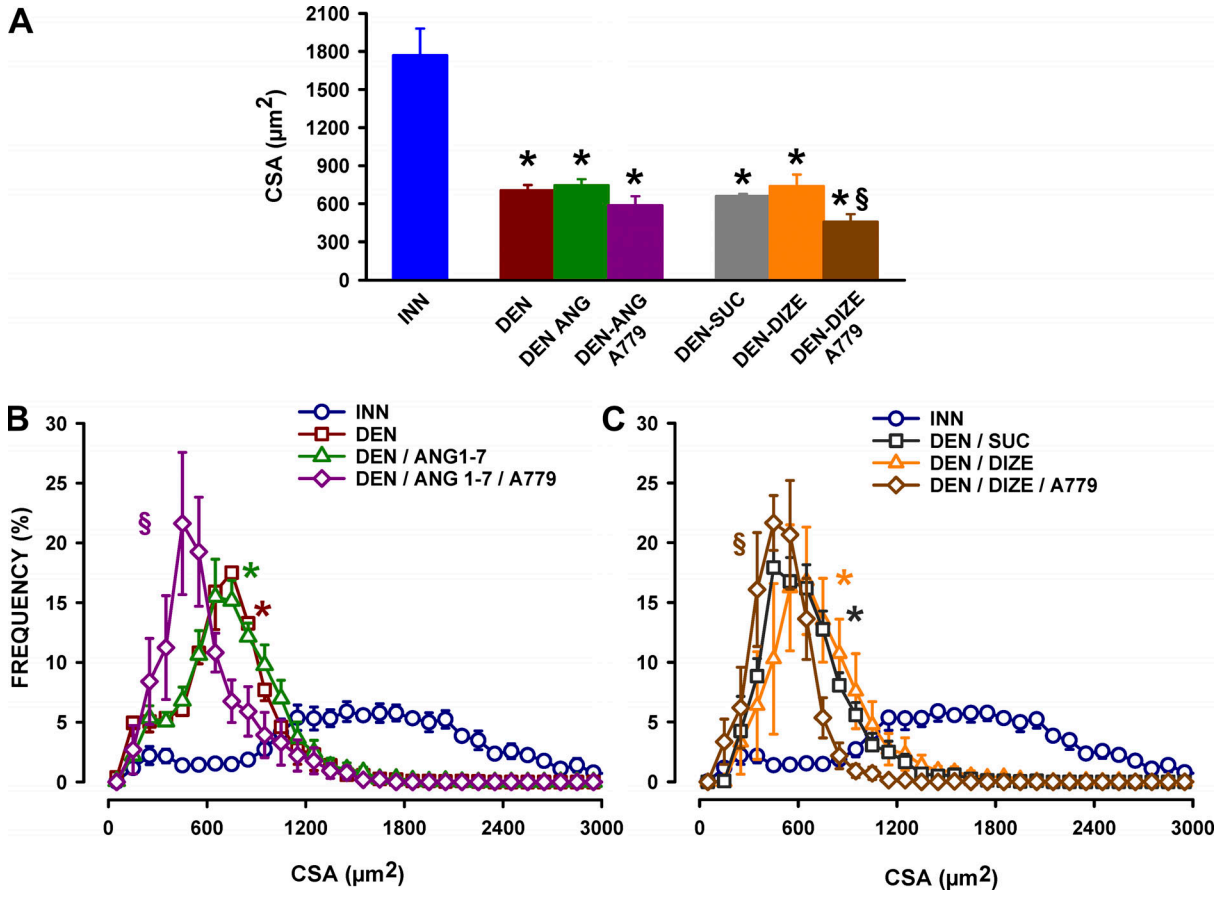

Figure 3. **Ang 1–7 did not prevent the decrease in fiber CSA associated with 28-d denervation, but A779 significantly worsened the decrease in CSA in soleus.** (A) Mean fiber CSA values; fiber CSA distribution of (B) innervated, denervated soleus without or with Ang 1–7 treatment; (C) innervated, sucrose-treated, and DIZE-treated denervated soleus. CSA values were divided in bin of 100 µm^2, and the number of fibers in each bin is presented as a percentage of the total number of fibers analyzed. The CSA frequency distribution was first determined for each muscle, and then mean and SE (vertical bars) were calculated from four or five muscles (with a total number of fibers ranging between 1,970 and 3,850). *, CSA distribution was significantly shifted toward lower CSA when compared with innervated; §, CSA distribution was significantly shifted toward lower CSA when compared with denervated or denervated/sucrose (ANOVA and LSD, $P < 0.05$).

blocking reagent and washed with PBS. Cross sections were incubated 5 min in a MOM diluent protein concentrated solution before being exposed for 1 h to mouse monoclonal anti-myosin type I (A4.840), anti-myosin IIA (SC-71), or anti-myosin heavy chain type IIB (BF-F3; Developmental Studies Hybridoma Bank). After three washouts with PBS, cross sections were exposed for 10 min to biotinylated anti-mouse IgG reagent solution. Finally, cross sections were incubated for 15 min in a fluorescein avidin solution (1:500) followed by three washouts in PBS. Laminin staining was done by incubating cross sections with anti-laminin antibody (1:1,000, catalog no. L9393, rabbit polyclonal; MilliporeSigma, Canada) for 30 min followed by Alexa Fluor 594 (1:500, catalog no. A-11012; Invitrogen). After three washouts with PBS, sections were mounted on slides with mounting media and covered with a coverslip. Images were captured on a Zeiss Axiolmager.M2 microscope using a digital camera (AxioCam mRm CCD). Pictures were taken from overlapping regions of each muscle and then collaged together to allow fiber typing and CSA (from the laminin boundaries) measurements from all fibers of each muscle using Imaris software (Bitplane).

Western blot analysis

EDL and soleus muscles were freeze-clamped in liquid nitrogen and kept at −80°C until use. Muscles were homogenized in Tris lysis buffer containing 20 mM HEPES, 10 mM NaCl, 1.5 mM MgCl, 1 mM dithiothreitol, 20% glycerol, 0.1% Triton X-100, and a cocktail of protease inhibitors (catalog no. 04693124001; MilliporeSigma, Canada) and phosphatase inhibitors (catalog no. 04693124001; MilliporeSigma, Canada). Homogenates were centrifuged for 10 min at 1,200 *g* and 4°C. Protein concentrations in the supernatants were determined using the bicinchoninic acid assay method (Thermo Fisher Scientific). The final protein concentrations were adjusted using Laemmli buffer (45 SDS, 20% glycerol, 10% β mercaptoethanol, 0.004% bromophenol blue, and 0.125 M Tris HCl, pH 6.8) to 25 µg/10 ml and heated for 5 min at 95°C. Proteins (25 µg/10 µl) were subjected to 8% SDS/PAGE, transferred onto a nitrocellulose membrane (Miniprotean III apparatus; Bio-Rad), and probed with the following primary antibodies: rabbit anti-total-Akt (T-Akt; catalog no. 4691), rabbit anti-phospho-Akt (P-Akt; catalog no. 4060), rabbit anti-total 4EPB (catalog no. 9452), rabbit anti-phospho-4EPB (P-4EBP;

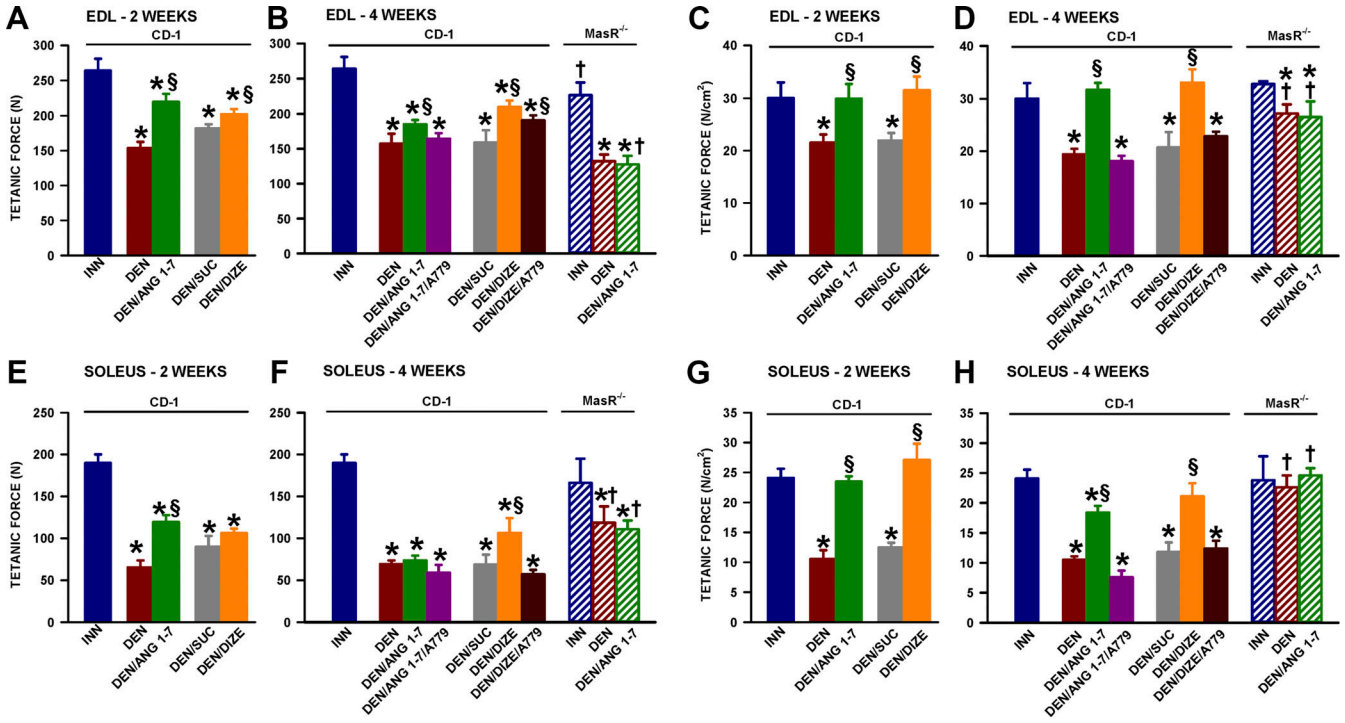

Figure 4. **Ang 1–7 and DIZE significantly prevented the loss of tetanic force in CD-1 EDL and soleus associated with 14- and 28-d denervation periods.** Tetanic force in N of EDL after (A) 2-wk and (B) 4-wk denervation; of soleus at (E) 2-wk and (F) 4-wk denervation, normalized to CSA in N/cm^2 for EDL at (C) 2-wk and (D) 4-wk denervation, for soleus at (G) 2-wk and (H) 4-wk denervation. Tetanic force represents the maximum force a muscle can generate and was measured at 200 Hz. Vertical bars represent the SE of five or six muscles. *, Mean tetanic force significantly different from that of innervated muscles; §, mean tetanic force significantly different from that of denervated or denervated/sucrose muscles; †, mean tetanic force significantly different from that of CD-1 muscles (ANOVA and LSD, $P < 0.05$).

catalog no. 9452), rabbit anti-Na-K pump α1 subunit (catalog no. 3010S; Cell Signaling Technology), rabbit anti-MuRF-1 (catalog no. 554561AP; Cedarlane), rabbit anti-total S6 (catalog no. Ab32529; Abcam), rabbit anti-Atrogin-1 (catalog no. AP2041; ECM Bioscience), mouse anti-phospho-S6 (P-S6; catalog no. MABS82), rabbit anti-Na-K pump α2 subunit (catalog no. 07674; MilliporeSigma, Canada), rabbit anti-α-actin (catalog no. CSBPA00750E0RB), and mouse anti-total myosin (catalog no. MAB4470; Cedarlane). Horseradish peroxidase–conjugated secondary antibodies, either goat anti-rabbit antibody (catalog no. 7074; Cell Signaling Technology) or goat anti-mouse antibody (catalog no. G21040; Thermo Fisher Scientific), were then used for visualization. Immunoreactions were visualized and quantified by chemiluminescence ECL (PerkinElmer) using the LI-COR imaging system (model no. 2800).

Statistical analysis

Data are expressed as mean ± SE. One-way ANOVA was used to determine statistical differences for twitch and tetanic force, frequency 50, excitability, resting E_M, overshoot, protein content measured by Western blot, muscle weight, and CSA. Calculations were made using the general linear model procedures of Statistical Analysis Software (SAS Institute). When a main effect or an interaction was significant, the least square difference (LSD) was used to locate significant differences (Steel and Torrie, 1980). The word "significant" refers only to a statistical difference ($P < 0.05$).

Results

Muscle weight and CSA

EDL and soleus muscle weight per se (data not shown) or expressed as a ratio of body weight (Fig. 1) gave rise to similar results. EDL muscle to body weight ratio did not significantly decrease during the first 3 d of denervation (Fig. 1 A), whereas a significant 17% decrease occurred for the soleus (Fig. 1 C). Neither Ang 1–7 nor DIZE altered muscle weight loss. Muscle to body weight ratio further decreased over the 14- and 28-d denervation period, with decreases after 28 d being 38% and 48% for EDL and soleus, respectively. Treating mice with Ang 1–7 had no significant effect on the weight ratio. DIZE-treated muscles, on the other hand, had significantly higher weight ratios than denervated sucrose-treated muscles; the significant effects occurred only for the 14-d denervation period for EDL and both 14- and 28-d period for soleus; for the latter muscle, A779, a MasR antagonist, inhibited the DIZE effect at 28 d. Body weight ratios were greater for MasR$^{-/-}$ EDL and especially soleus muscle than for CD-1 muscles (Fig. 1, B and D). The loss of muscle weight over a 28-d denervation period was 52% and 48% for EDL and soleus, respectively. Treating MasR$^{-/-}$ mice with Ang 1–7 did not affect the extent of muscle weight loss.

To specifically determine how Ang 1–7 affects muscle fibers, we next measured fiber CSA. Mean EDL fiber CSA decreased by 32% during a 28-d denervation period (DEN and DEN/SUC in Fig. 2 A). The extent of the decreases in CSA was not altered when mice were treated with either Ang 1–7 or DIZE.

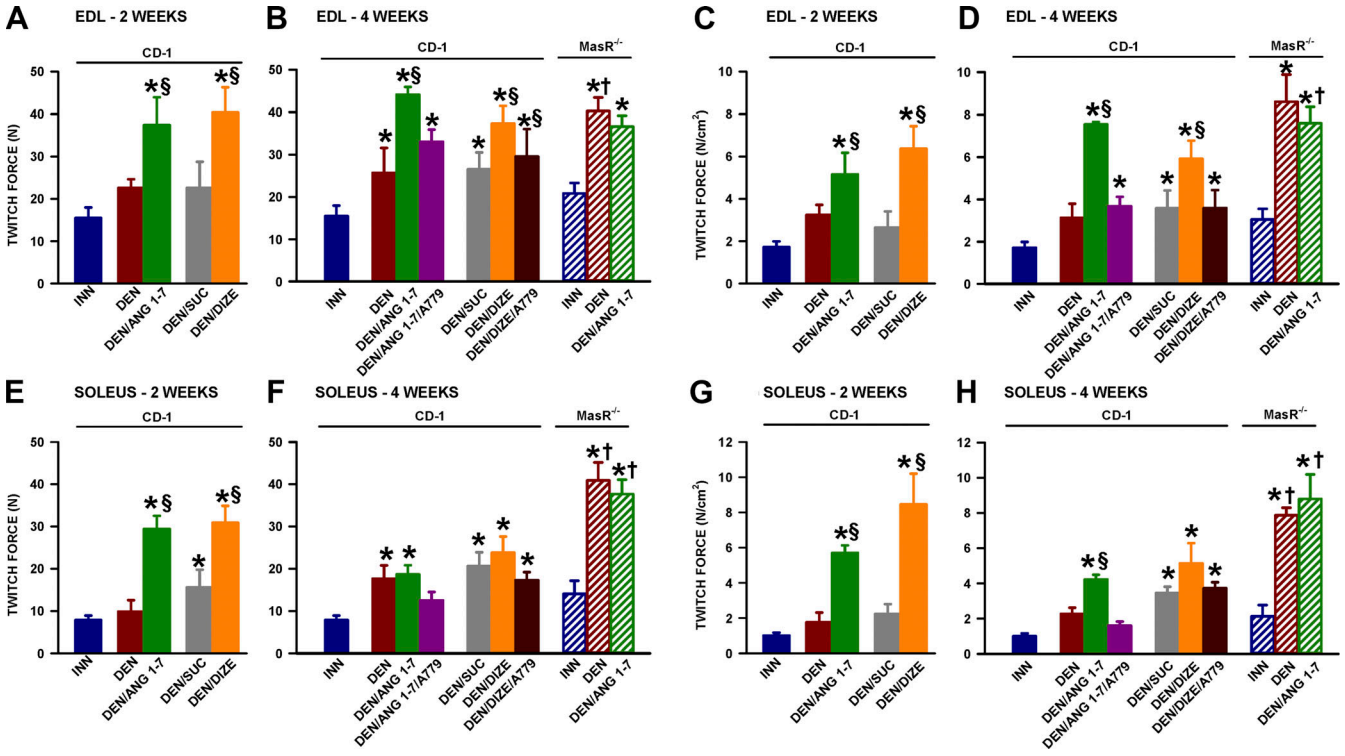

Figure 5. **Ang 1–7 and DIZE significantly increased twitch force of CD-1 EDL and soleus associated with 14- and 28-d denervation periods, but not in MasR$^{-/-}$ muscles.** Twitch force in N of EDL after (A) 2-wk and (B) 4-wk denervation; of soleus at (E) 2-wk and (F) 4-wk denervation, normalized to CSA in N/cm^2 for EDL at (C) 2-wk and (D) 4-wk denervation, for soleus at (G) 2-wk and (H) 4-wk denervation. Vertical bars represent the SE of five muscles. *, Mean twitch force significantly different from that of INN muscle; §, mean twitch force significantly different from that of denervated or denervated/sucrose muscle; †, mean twitch force significantly different from that of wild-type soleus (ANOVA and LSD, $P < 0.05$).

Denervation significantly reduced the proportion of fibers with CSA >1,500 μm^2 while it significantly increased the proportion of fibers with CSA below 1,200 μm^2 (Fig. 2 B). Ang 1–7, DIZE, and A779 (data not shown for the latter) did not affect the CSA frequency distribution (Fig. 2, B and C). The effects of denervation, Ang 1–7, and DIZE on soleus fiber CSA (Fig. 3) were very similar to those of EDL, with three exceptions: (1) 28-d denervation reduced soleus fiber CSA by 61% compared with only 32% in EDL, (2) the shift toward lower CSA in the CSA distribution was much more pronounced in soleus, and (3) A779 significantly exaggerated the CSA loss in soleus muscle, but not in EDL.

Tetanic and twitch force

As EDL became smaller over the 14- and 28-d denervation period, mean tetanic forces in newton (N) decreased significantly when compared with their innervated counterpart (Fig. 4, A and B). Mean tetanic forces of Ang 1–7– or DIZE-treated denervated EDL were significantly greater compared with that of untreated denervated EDL but remained significantly less than that of innervated EDL. However, when tetanic forces were normalized to CSA, EDL mean tetanic forces from Ang 1–7– and DIZE-treated denervated EDL were no longer significantly different from that of innervated EDL, while those of untreated denervated EDL were still significantly less (by 36%; Fig. 4, C and D). Thus, both Ang 1–7 and DIZE fully prevented the loss of normalized tetanic force associated with denervation, an effect completely inhibited by A779. MasR$^{-/-}$ EDL mean tetanic force (in newton) also decreased during a 28-d denervation period, a decrease that was similar to that of CD-1 EDL (Fig. 4 B). However, when tetanic force was normalized to CSA, mean tetanic force of denervated MasR$^{-/-}$ EDL decreased by only 17% compared with 36% in CD-1 denervated EDL (Fig. 4 D). Ang 1–7 did not allow for an increased in normalized tetanic force during a 28-d denervation period as it did for CD-1 EDL.

Similarly, all denervated soleus mean tetanic forces (in N) were significantly lower than those in innervated soleus (Fig. 4, E and F), whereas the CSA normalized mean tetanic forces of Ang 1–7/DIZE–treated, but not untreated, denervated soleus remained similar to those of innervated soleus (Fig. 4, G and H). Again A779 completely blocked the Ang 1–7/DIZE effect. For MasR$^{-/-}$ soleus, 28-d denervation resulted in lower mean tetanic force in N (Fig. 4 F) but notably no loss in the CSA normalized tetanic force whether or not mice were Ang 1–7 treated (Fig. 4 H).

14- and 28-d denervated EDL generated greater mean twitch forces (in N or N/cm^2) than innervated EDL (Fig. 5, A–D). At 28-d denervation and compared with innervated EDL, the normalized twitch forces were 1.8- and 2.1-fold greater for denervated and sucrose-treated denervated EDL, respectively (DEN/SUC in Fig. 5 C). Ang 1–7– and DIZE-treated denervated EDL generated even greater twitch force than untreated denervated EDL; mean normalized twitch forces of Ang 1–7– and DIZE-treated EDL were respectively 4.4- and 3.5-fold greater than that of innervated EDL. The Ang 1–7 and DIZE effects were

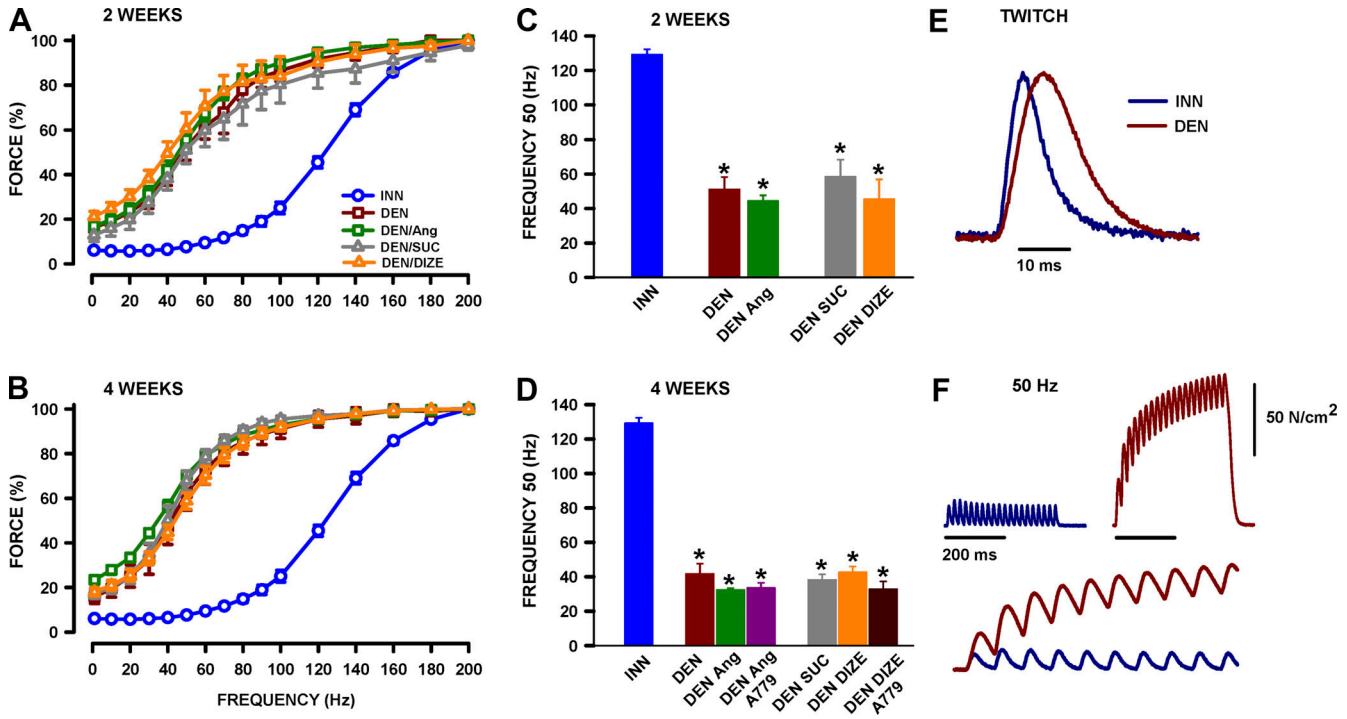

Figure 6. **In CD-1 EDL, Ang 1–7 did not prevent the shift in the force–frequency relationship toward lower stimulation frequencies that occurred after 14 and 28 d of denervation. (A and B)** Force–frequency relationships at (A) 2-wk and (B) 4-wk denervation. Forces are expressed as a percentage of the force measured at 200 Hz. **(C and D)** Frequency 50 at (C) 2-wk and (D) 4-wk denervation. Frequency 50 is the stimulation frequency at which force was 50% of the maximum tetanic force (see Materials and methods for calculations). **(E)** Examples of twitch force traces from innervated and denervated muscles. Forces are plotted as a percentage of the maximum force during contraction. **(F)** Example of force traces elicited at 50 Hz from innervated and denervated muscle. Horizontal bars show the 200-ms portions of the contractions that are expanded below. Vertical bars (A and B) represent the SE of five muscles. *, Mean frequency 50 significantly different compared with innervated muscle (ANOVA and LSD, $P < 0.05$).

completely blocked by A779 (Fig. 5, B and D). Innervated MasR$^{-/-}$ EDL mean normalized twitch force was 1.8 times greater than that of innervated CD-1 EDL. For MasR$^{-/-}$ EDL, mean twitch force after 28-d denervation became 2.8 times greater than in innervated MasR$^{-/-}$ EDL, an effect much greater when compared with wild-type EDL, for which the difference was only 1.8-fold. Ang 1–7 did not cause any further increase in twitch force of denervated MasR$^{-/-}$ EDL. Denervation, Ang 1–7, DIZE, and A779 effects in soleus were similar to those described for EDL for both CD-1 and MasR$^{-/-}$ soleus (Fig. 5, E–H).

14- and 28-d denervation was also associated with a significant shift in the CD-1 EDL force–frequency relationship toward lower stimulation frequencies, and this shift was not prevented by Ang 1–7 or DIZE (Fig. 6, A–D). The shift occurred as twitch contractions became slower (Fig. 6 E), with mean times to peak and half-relaxation times becoming significantly longer in denervated muscles (Table 1). As a consequence of prolonged twitch contractions, stimulation at 50 Hz still resulted in individual twitches in innervated EDL, while there was a clear summation of twitch contractions in denervated EDL (Fig. 6 F). Wild-type EDL time to peak and half-relaxation time during tetanic contractions also became significantly prolonged following 28-d denervation (Table 2). Neither Ang 1–7 (Tables 1 and 2) nor DIZE (data not shown) reversed the denervation effects on time to peak and half-relaxation time. Similar to wild-type EDL, the force–frequency relationship of denervated soleus was significantly shifted toward lower stimulation frequencies (Fig. 7). Contrary to EDL, however, the shift was slightly accentuated by Ang 1–7 and DIZE, especially at 14-d denervation. Soleus twitch contractions also became significantly longer with prolonged time to peak and half-relaxation time, and these effects were not reversed by Ang 1–7 (Table 1) or DIZE (data not shown). For tetanic contractions, time to peak was not affected, while half-relaxation times were significantly longer in wild-type denervated than innervated soleus (Table 2).

Although 28-d denervation had small effects on tetanic force loss in MasR$^{-/-}$ than in wild-type EDL and soleus, significant shifts of the force–frequency relationship toward lower stimulation frequencies were observed in denervated compared with innervated MasR$^{-/-}$ muscles (Fig. 8). Ang 1–7 did not accentuate the shift in MasR$^{-/-}$ soleus. Again, the shift in the force–frequency relationship was linked to prolonged twitch contractions, as both time to peak and half-relaxation time were significantly longer in denervated than innervated EDL and soleus (Table 1). Notably, mean half-relaxation time of denervated MasR$^{-/-}$ EDL and soleus were significantly longer than those of denervated wild-type EDL and soleus. Longer tetanic contraction times to peak and half-relaxation times were also observed in denervated than in innervated MasR$^{-/-}$ EDL, whereas only half-relaxation times were significantly longer in denervated MasR$^{-/-}$ soleus (Table 2).

Table 1. **Ang 1–7 does not reverse the significant prolongation of twitch contraction associated with 4-wk denervation for both wild-type and MasR$^{-/-}$ EDL and soleus**

Muscle	Condition	Wild type		MasR$^{-/-}$	
		Time to peak (ms)	Half-relaxation time (ms)	Time to peak (ms)	Half-relaxation time (ms)
EDL	Innervated	7.2 ± 1.1	5.8 ± 0.3	8.2 ± 0.8	10.2 ± 1.2
EDL	Denervated	14.8 ± 1.4[a]	9.4 ± 1.1	13.4 ± 0.8[a]	17.0 ± 1.5[a,b]
EDL	Denervated Ang 1–7	13.0 ± 1.1[a]	11.9 ± 0.7[a]	17.3 ± 4.2[a,b]	20.5 ± 5.3[a,b]
Soleus	Innervated	15.7 ± 0. 6	10.3 ± 1.1	13.3 ± 0.7	16.6 ± 2.24
Soleus	Denervated	33.7 ± 1.0[a]	38.5 ± 4.9[a]	28.9 ± 1.7[a]	43.9 ± 4.5[a]
Soleus	Denervated Ang 1–7	34.7 ± 1.1[a]	37.2 ± 2.7[a]	25.3 ± 3.5[a,b]	35.6 ± 9.1[a]

Ang 1–7 was delivered using an osmotic pump at a rate of 15 mg/kg/d. Data are presented as mean ± SE of five or six muscles.
[a]Mean value is significantly different from that of innervated muscles (ANOVA and LSD, $P < 0.05$).
[b]Mean value is significantly different from CD-1 muscles (ANOVA and LSD, $P < 0.05$).

Table 2. **Ang 1–7 does not reverse the prolongation of the tetanic time to peak in EDL and half-relaxation time of EDL and soleus associated with 4-wk denervation in both wild-type and MasR$^{-/-}$ mice**

Muscle	Condition	Wild type		MasR$^{-/-}$	
		Time to peak (ms)	Half-relaxation time (ms)	Time to peak (ms)	Half-relaxation time (ms)
EDL	Innervated	118.8 ± 11.0	19.0 ± 2.9	118.5 ± 22.2	27.8 ± 1.4
EDL	Denervated	196.9 ± 3.8[a]	44.8 ± 2.7[a]	178.4 ± 18.7[a]	53.4 ± 3.0[a]
EDL	Denervated Ang 1–7	197.4 ± 2.7[a]	45.2 ± 2.5[a]	191.7 ± 8.4[a]	63.8 ± 13.1[a,b]
Soleus	Innervated	204.6 ± 0.7	43.3 ± 1.7	211.8 ± 1.2	52.3 ± 3.6
Soleus	Denervated	208.0 ± 6.0	95.3 ± 5.9[a]	213.4 ± 1.4	103.8 ± 10.2[a]
Soleus	Denervated Ang 1–7	210.0 ± 5.3	97.6 ± 11.7[a]	212.0 ± 5.0	85.2 ± 11.3[a]

Ang 1–7 was delivered using an osmotic pump at a rate of 15 mg/kg/d. Tetanic contractions for EDL and soleus were respectively elicited at 200 and 140 Hz. Data are presented as mean ± SE of five or six muscles.
[a]Mean value is significantly different from that of innervated muscles (ANOVA and LSD, $P < 0.05$).
[b]Mean value is significantly different from CD-1 muscles (ANOVA and LSD, $P < 0.05$).

Membrane excitability, resting E_M, and action potential

It is well established that the sarcolemma of denervated muscle fibers are depolarized (Albuquerque and Thesleff, 1968; Albuquerque et al., 1971; Wareham, 1978; Clausen et al., 1981). Thus, we next tested whether Ang 1–7 improves resting E_M as a potential physiological mechanism that prevents the loss of normalized tetanic force following denervation. Fiber excitability was 100% in innervated EDL, as all fibers generated an action potential upon a single stimulation (Fig. 9 A). After a 28-d denervation period, fiber excitability fell to 42–49% (DEN and DEN-SUC). Ang 1–7 treatment completely prevented the loss of fiber excitability, while excitability was 85% in DIZE-treated denervated EDL. As previously reported, denervated fibers were significantly depolarized compared with innervated fibers, with a mean resting E_M of −62 mV for denervated fibers versus −76 mV for innervated fibers (Fig. 9 B). Both Ang 1–7 and DIZE significantly, but not completely, reduced the extent of depolarization in denervated EDL fibers, with a mean resting E_M of −69 mV. Mean overshoots were significantly less in denervated than innervated fibers, an effect completely prevented by Ang 1–7 and DIZE (Fig. 9 C). Mean maximum rates of depolarization of denervated fibers were 2.2- to 2.7-fold less than in innervated fibers; however, for this parameter, neither Ang 1–7 nor DIZE significantly abolished the denervation effect (Fig. 9 D). The effects of denervation, Ang 1–7, and DIZE in soleus were basically similar to those of wild-type and MasR$^{-/-}$ EDL (Fig. 9, E–H).

Considering that the normalized mean tetanic forces of MasR$^{-/-}$ EDL and soleus were less affected by denervation than their CD-1 counterpart and that Ang 1–7 fully prevented the loss of membrane excitability and normalized tetanic force, we also determined the effect of denervation on fiber excitability of MasR$^{-/-}$ EDL and soleus. Although mean fiber excitability and resting E_M significantly decreased during the 28-d denervation compared with innervated muscles, the extent of the decreases was less in MasR$^{-/-}$ than in CD-1 muscles. Contrary to CD-1, mean action potential overshoot was completely abolished in denervated MasR$^{-/-}$ EDL and soleus, as the mean action potential peaks were respectively −8 and −4 mV.

Fiber excitability is suppressed when resting E_M becomes less negative than approximately −60 mV (Cairns et al., 1995; Ammar et al., 2015). So, to better understand how the reduced resting E_M depolarization with Ang 1–7/DIZE affected membrane excitability, we determined the frequency distribution of resting E_M. For innervated EDL, resting E_M ranged from −90 to −60 mV (Fig. 10 A; i.e., none of the fibers were in the unexcitable range). The resting E_M distribution of denervated fibers was significantly shifted toward less negative E_M, and up to 35% of the fibers had resting E_M less negative than −60 mV. Ang 1–7 significantly shifted the resting E_M distribution toward more negative E_M, reducing the number of fibers with resting E_M less negative than −60 mV to 0. A similar situation was observed with DIZE, except that the number of fibers with resting E_M less negative than −60 mV was 11% (Fig. 10 B), in agreement with the decrease in fiber excitability still detectable (Fig. 9 A). The effects of denervation, Ang 1–7, and DIZE in soleus were basically similar to those of EDL (Fig. 10, C and D).

The membrane depolarization associated with denervation is due to an increased Na^+ permeability and decreased K^+

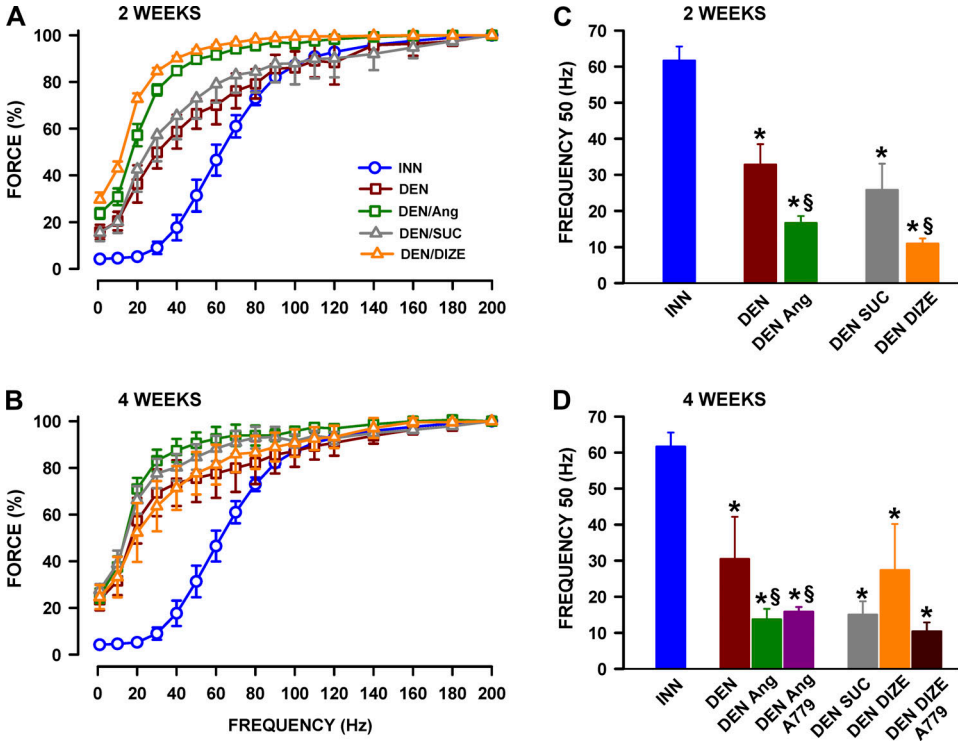

Figure 7. **In CD-1 soleus, Ang 1–7 did not prevent the shift of the force–frequency relationship toward lower stimulation frequencies following 14 and 28 d of denervation. (A and B)** Force–frequency relationships at (A) 2-wk and (B) 4-wk denervation. Forces are expressed as a percent of the force at 200 Hz. **(C and D)** Frequency 50 at (C) 2-wk and (D) 4-wk denervation. Frequency 50 is the stimulation frequency at which force was 50% of the maximum tetanic force (see Materials and methods for calculations). Vertical bars represent SE of five muscles. *, Mean frequency 50 significantly different from that of innervated muscles; §, mean frequency 50 significantly different from that of denervated or denervated/sucrose muscle soleus (ANOVA and LSD, $P < 0.05$).

permeability (Kotsias and Venosa, 1987). The Na^+ K^+ pump content, which contributes up to −15 mV to the resting E_M in innervated muscles (Chibalin et al., 2012; Ammar et al., 2015), also decreases during denervation (Clausen et al., 1981; Clausen et al., 1982; Ward et al., 1987). So, we measured the Ang 1–7 effects on the pump α1 and α2 subunit protein content over a 28-d denervation period. Denervated EDL had significantly greater α1 and α2 protein content than innervated EDL, the differences being 1.8- and 1.5-fold, respectively (Fig. 11, A and B). The increase in α1 reached 2.9- and 2.3-fold for Ang 1–7 and DIZE treatment, respectively. Ang 1–7 also increased the α2 protein content by 2.0-fold when compared with innervated EDL. Contrary to the situation in EDL, 28-d denervation resulted in significant decreases in both α1 and α2 content by 40–50%, while neither Ang 1–7 nor DIZE had any effect.

Contractile components

Denervation also leads to decreases in sarcomere contents, especially near the cell membrane within 14 d (Yang et al., 2020). We therefore determined the total α-actin and myosin content to document whether Ang 1–7 reduces the loss of contractile proteins during the 28-d denervation period. α-Actin protein content was reduced by 12% in denervated EDL, while Ang 1–7 and DIZE had no effect (Fig. 11 C). Denervation caused greater decreases in α-actin in soleus, as the content was reduced by 30%. Although no decrease in α-actin was detected with Ang 1–7, the difference with denervated soleus was not significant, while DIZE had no effect. Ang 1–7 and DIZE caused decreases in total myosin content, even when denervation alone had a small effect (Fig. 11 D).

Normal innervated EDL muscle contained 60% type IIB, 15% type IIA, and 2% type I fibers (Fig. 12). After 28-d denervation, the proportion of fibers expressing type I and IIA myosin significantly increased in EDL muscle to 7% and 96%, respectively, while the number of fibers expressing type IIB myosin did not change. However, as shown in Fig. 12 A, while a large number of denervated fibers still expressed type IIB myosin, the intensity of the staining is much less in denervated than innervated fibers. Ang 1–7 partially reduced the increase in the number of fibers to 4% for the expression of type I myosin and 54% for type IIA myosin. Contrary to EDL, innervated soleus muscle contain 62% type I fibers and 44% type IIA fibers (Fig. 13). Neither denervation nor Ang 1–7 significantly affected the fiber type composition in soleus.

Hypertrophic and atrophic pathways

Total Akt (T-Akt) and phosphorylated Akt (P-Akt) protein content was significantly greater after 14 and 28 d of denervation, but not after 3 d, when compared with levels in innervated EDL (Fig. 14, A and B). Neither Ang 1–7 nor DIZE affected T-Akt and P-Akt content. T-4EBP and P-4EBP slightly increased after 3 and 14 d of denervation followed by a decrease at 28 d (Fig. 14, C and D). Ang 1–7 had only one significant effect, as it increased T-4EBP at 3 d. Significant increase in P-S6 content was observed

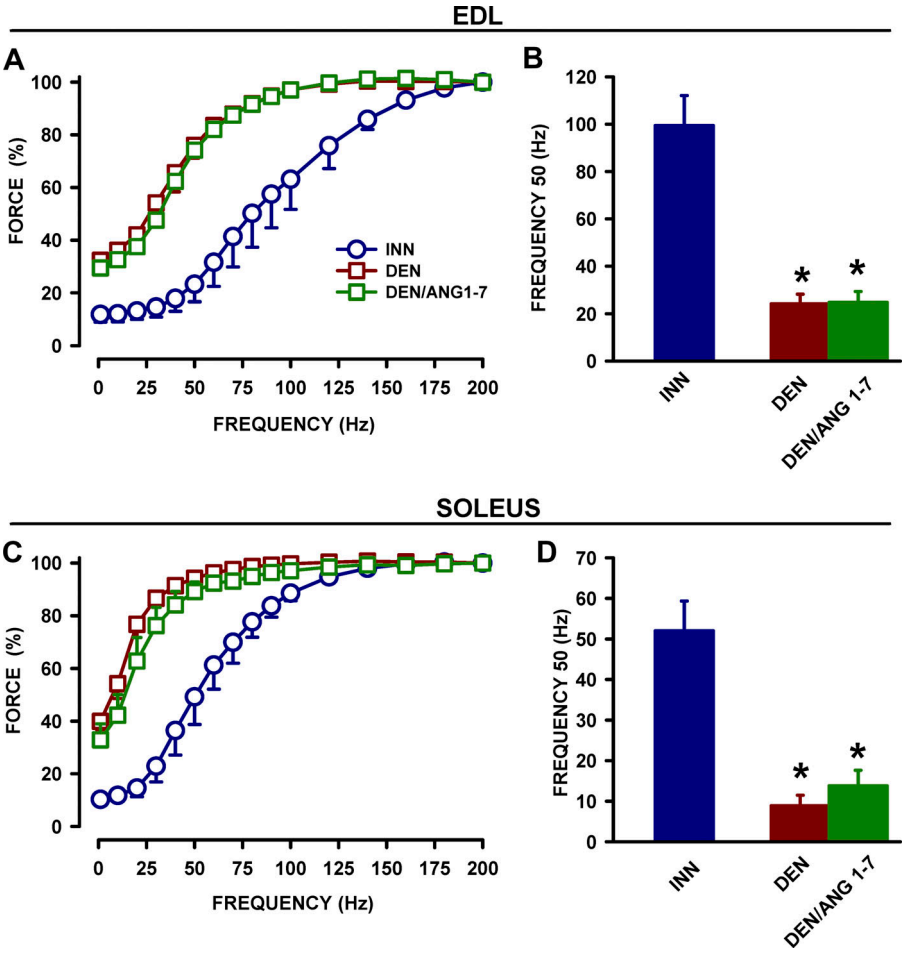

Figure 8. **Force–frequency relationships of MasR$^{-/-}$ EDL and soleus were significantly shifted toward lower stimulation frequencies after a 28 d denervation period. (A and C)** Force-frequency relationships of (A) EDL and (C) soleus. Forces are expressed as a percentage of the force at 200 Hz. Frequency 50 of (B) EDL and (D) soleus. Frequency 50 is the stimulation frequency at which force was 50% of the maximum tetanic force (see Materials and methods for calculations). Vertical bars represent SE of five muscles. *, Mean frequency 50 significantly different compared with innervated muscle (ANOVA and LSD, $P < 0.05$).

only at 14-d denervation, without any effect of Ang 1–7 or DIZE (Fig. 14, E and F). In soleus, denervation significantly increased T-Akt content at 14 d; there were also increases in P-Akt content at 14 and 28 d, but the differences compared with innervated muscle were not significant (Fig. 15, A and B). There were no significant changes in T-4EPB and P-4EPB as well as for rabbit anti-total S6 and P-S6 (Fig. 15, C–F). Neither Ang 1–7 nor DIZE affected levels of Akt, 4EPB, and S6. Significant decreases in MuRF-1 protein content were observed in EDL at 28 d and insoleus at both 14 and 28 d (Fig. 16, A and B), while decreases in atrogin-1 were observed at both 14 and 28 d, being especially significant at 28 d (Fig. 16, B and C). Neither Ang 1–7 nor DIZE affected MuRF-1 and atrogin-1 levels.

Discussion

The major findings regarding changes in EDL and soleus during 14- and 28-d denervation periods were as follows. (1) Neither Ang 1–7 nor DIZE prevented the loss of muscle mass and fiber CSA. (2) Twitch force increased and was further potentiated by Ang 1–7 and DIZE. (3) Ang 1–7 and DIZE were fully effective at maintaining normalized maximal tetanic force. (4) A779, a MasR antagonist, fully blocked the effect of Ang 1–7 and DIZE on twitch and tetanic force. (5) Normalized tetanic force of MasR$^{-/-}$ EDL and soleus was less affected when compared with their wild-type counterpart, and Ang 1–7 did not potentiate twitch force. (6) Neither Ang 1–7 nor DIZE prevented the shift in force–frequency relationship in denervated EDL but caused a further shift in denervated soleus. (7) Ang 1–7 prevented the loss in membrane excitability, membrane depolarization, and decreases in action potential overshoot. (8) Na^+-K^+ pump protein content increased in EDL, an effect potentiated by Ang 1–7, whereas in soleus, denervation reduced pump content, while Ang 1–7 had no effect. (9) Ang 1–7 did not allow for an increase in α-actin and myosin content. (10) There was a shift in fiber type toward type I and IIA in denervated EDL muscle, an effect partially reversed by Ang 1–7, whereas fiber type composition of soleus was unaffected by denervation and Ang 1–7. (11) Ang 1–7 and DIZE had little effect on the protein content of total and phosphorylated Akt, 4EPB, and S6, three important hypertrophic factors, as well as little effect on MuRF-1 and atrogin-1 content.

Ang 1–7 maintains muscle function in denervated muscles, but not muscle mass

In regard to muscle mass, only DIZE significantly reduced the extent of mass loss. DIZE, at 15 mg/kg/d as in this study, increases plasma Ang 1–7 levels by almost fourfold (Zhang et al., 2015). At 350–390 ng/kg/min Ang 1–7, plasma and kidney levels increased by approximately twofold (Oh et al., 2012; Mori et al., 2014); so, at a dose of 100 ng/kg/d, as in this study, the increase

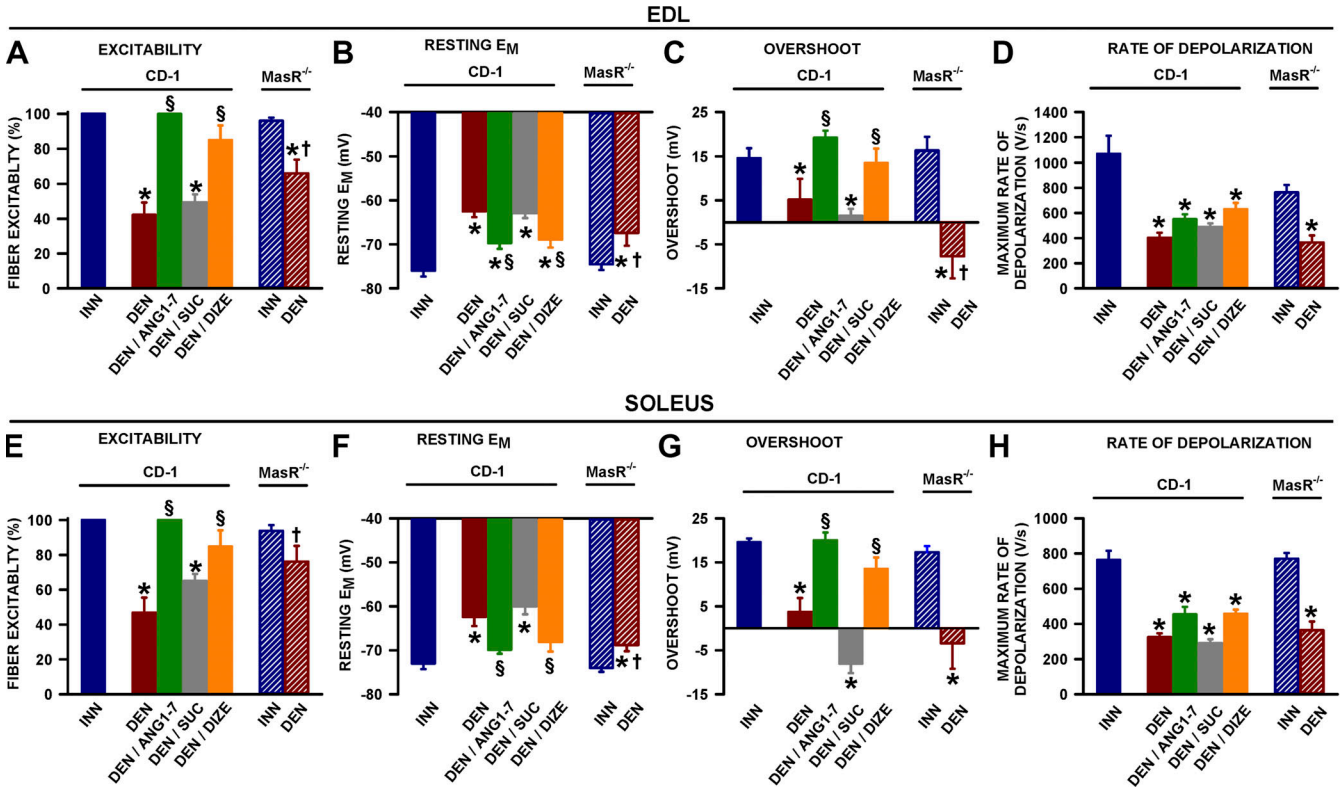

Figure 9. **Ang 1–7 significantly improved membrane excitability in 28-d denervated EDL and soleus.** (A) Fiber excitability, (B) resting E_M, (C) action potential overshoot, (D) rate of depolarization in EDL fibers, (E) fiber excitability, (F) resting E_M, (G) action potential overshoot, and (H) rate of depolarization in soleus fibers. Action potentials were triggered with a single stimulation. Excitability is defined as the number of fibers that generated an action potential upon stimulation and is expressed as a percentage of all tested fibers. Mean values from individual fibers were first averaged for each muscle, and mean and SE (vertical bars) were calculated from five or six muscles, with a total number of tested fibers ranging between 70 and 123. *, Mean value significantly different from that of innervated muscle; §, mean value significantly different from that of denervated or denervated/sucrose muscle; †, mean value for denervated $MasR^{-/-}$ muscles significantly different from mean value of denervated CD-1 muscles (ANOVA and LSD, $P < 0.05$).

in Ang 1–7 level is expected to be less than with DIZE. Although one can then suggest that at a high concentration Ang 1–7 has the capacity to reduce the extent of muscle mass loss during denervation, such conclusion is not supported by the results on fiber CSA, as neither Ang 1–7 nor DIZE prevented the reduction in fiber CSA. On the other hand, A779 worsened the reduction in fiber CSA in soleus, but not in EDL. The extent of muscle mass and force loss was greater in denervated soleus than EDL; that is, soleus is more sensitive to the denervation effect and perhaps is also more sensitive to a MasR inhibition, at least in terms of CSA reduction. We suggest that during denervation, endogenous Ang 1–7 helps at preventing fiber CSA decreases, primarily in soleus, because inhibiting the MasR worsened the decrease in fiber CSA, but a further increase in plasma Ang 1–7 levels (from either Ang 1–7 or DIZE treatment) was not effective at further reducing muscle fiber CSA loss.

Maximum tetanic force

As a consequence of muscle mass loss, the capacity of denervated muscles to generate force is drastically reduced whether it is expressed in N or normalized to CSA in N/cm^2 as previously reported (Finol et al., 1981). The decrease in normalized tetanic force suggests that the extent of the decrease exceeds the expected decrease from just a reduction in muscle mass. This study now demonstrates for the first time that Ang 1–7 completely prevents the loss of normalized tetanic force in both EDL and soleus. Ang 1–7 had little to no consistent effects on α-actin or myosin content, so the preservation of contractile proteins cannot be a mechanism for the maintenance of normalized force. However, future work should address the possibility that the myofibrillar fractional area could be altered in response to elevated Ang 1–7 levels. Another potential mechanism is a change in fiber type. In EDL, denervation leads to decreases in myosin IIB expression and increases in type IIA, an effect reversed by Ang 1–7. However, mouse and rat single type IIA and IIB fibers develop similar maximum force (Bottinelli et al., 1991; Pellegrino et al., 2003). Furthermore, neither denervation nor Ang 1–7 affects fiber type composition in soleus. It is therefore unlikely that changes in fiber type composition are involved in the preservation of normalized tetanic force in Ang 1–7–treated denervated muscles.

Mean resting E_M was much less negative in denervated than innervated muscle fibers as previously reported (Albuquerque and Thesleff, 1968; Albuquerque et al., 1971; Wareham, 1978; Clausen et al., 1981). Furthermore, a large proportion of denervated muscle fibers had resting E_M less negative than −60 mV, resting E_M at which muscle no longer generate force and thus action potential (Cairns et al., 1995; Ammar et al., 2015). The loss

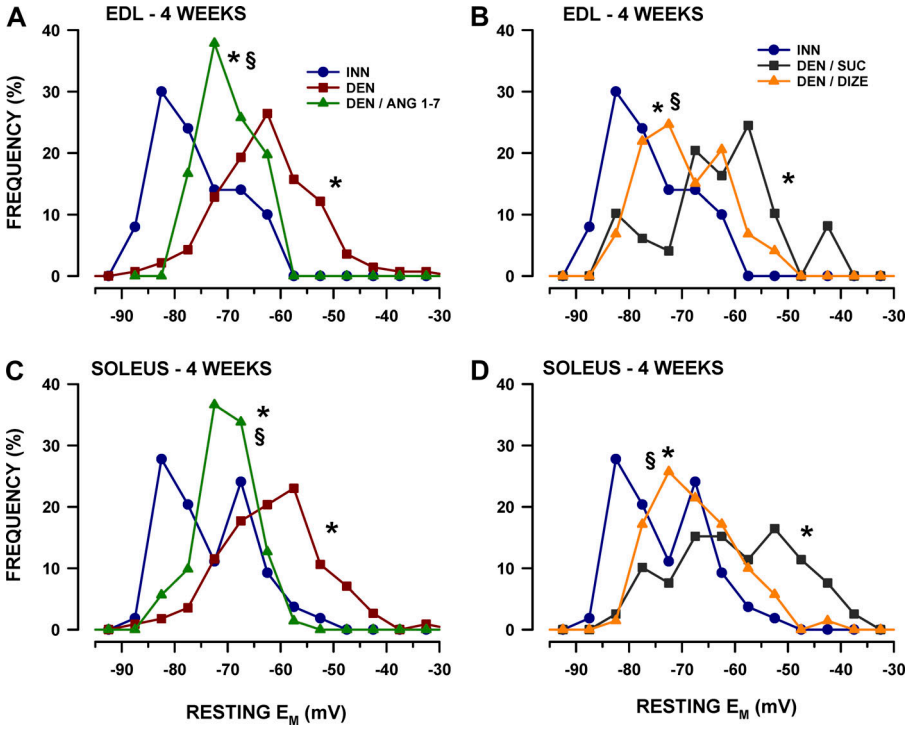

Figure 10. **Ang 1–7 partially shifted the resting E_M distribution of 28-d denervated CD-1 EDL and soleus toward that of innervated muscles.** Frequency distribution of resting E_M of (A) innervated, denervated, Ang 1–7 treated denervated EDL; (B) innervated, sucrose-treated, and DIZE-treated denervated EDL; (C) innervated, denervated, Ang 1–7 treated denervated soleus; (D) innervated, sucrose-treated, and DIZE-treated denervated soleus. Resting E_M values were divided in bin of 5 mV; the number of fibers from all muscles was counted for each bin and is expressed as a percentage of the total number of fibers tested. Total number of samples used for the distribution was 70–123 fibers from five or six muscles. *, Resting E_M distribution significantly shifted compared with that of innervated muscle; §, resting E_M distribution significantly shifted compared with that of denervated or denervated/sucrose muscle (Fisher test, $P < 0.05$).

of membrane excitability was completely prevented by Ang 1–7 and almost completely prevented by DIZE. Although mean resting E_M of Ang 1–7– or DIZE-treated denervated muscle fibers was still less negative compared with those of innervated fibers, none of the Ang 1–7–treated fibers had resting E_M less negative than −60 mV. For those treated with DIZE, a small number of fibers had resting E_M less negative than −60 mV, which is in agreement that a few fibers were still unexcitable. Finally, action

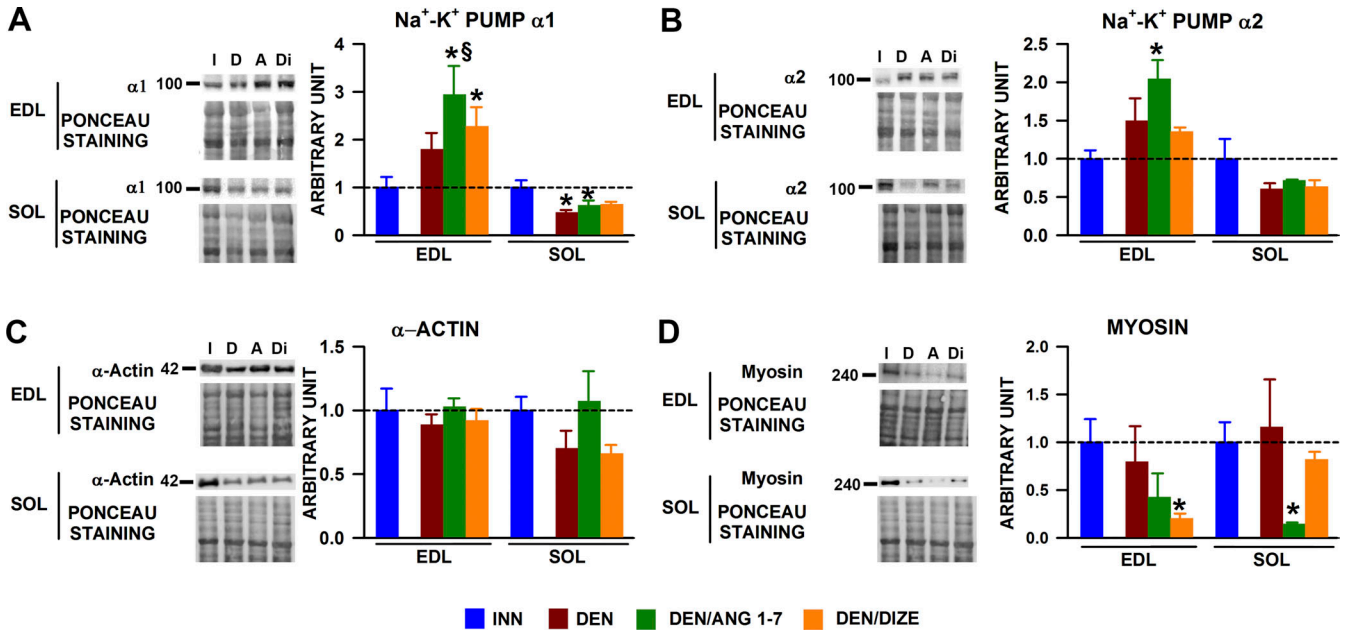

Figure 11. **Ang 1–7 significantly increased the Na^+ K^+ pump protein content in CD-1 EDL, but not the α-actin and myosin content after a 28-d denervation period.** Protein content of (A) Na^+-K^+ pump α1, (B) Na^+-K^+ pump α2, (C) α-actin, and (D) myosin. Ponceau staining is from the 3-d Western blots to provide an example for total proteins. A, denervated Ang 1–7 treated; D, denervated; Di, denervated-DIZE treated; I, innervated; SOL, soleus. The same blot was used to determine soleus actin and myosin content at 3 d, so images of Ponceau staining are the same for both proteins. Vertical bars represent the SE of six to eight muscles. *, Mean value significantly different from that of INN muscle; §, mean value significantly different from that of denervated muscle (ANOVA and LSD, $P < 0.05$).

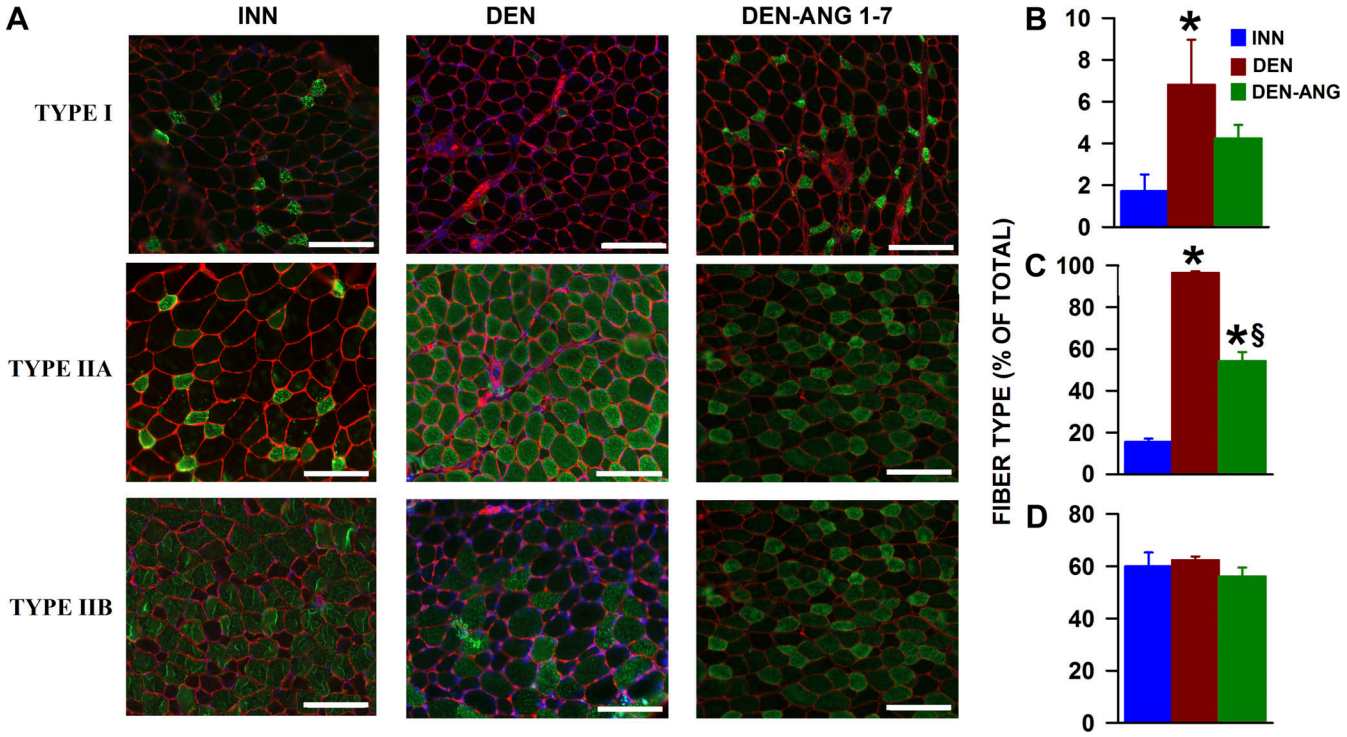

Figure 12. **Denervation significantly increased the expression of myosin I and IIA in CD-1 EDL, while Ang 1–7 partially reduced that effect. (A)** Images of type I, IIA, and IIB fibers in innervated, denervated, and denervated Ang 1–7–treated EDL (DEN-ANG 1–7). **(B–D)** The number of fibers expressing myosin I (B), myosin IIA (C), and myosin IIB fibers (D) is expressed as a percentage of the total number of fibers. Percent values were calculated for each muscle, and then mean and SE (vertical bars) were calculated from four or five muscles. Scale bars, 100 µm. The total number of fibers analyzed for innervated, denervated, and DEN-Ang 1–7 were 3,293, 4,144, and 4,321, respectively. *, Mean value significantly different from that of innervated muscle; §, mean value significantly different from that of denervated muscle (ANOVA and LSD, $P < 0.05$).

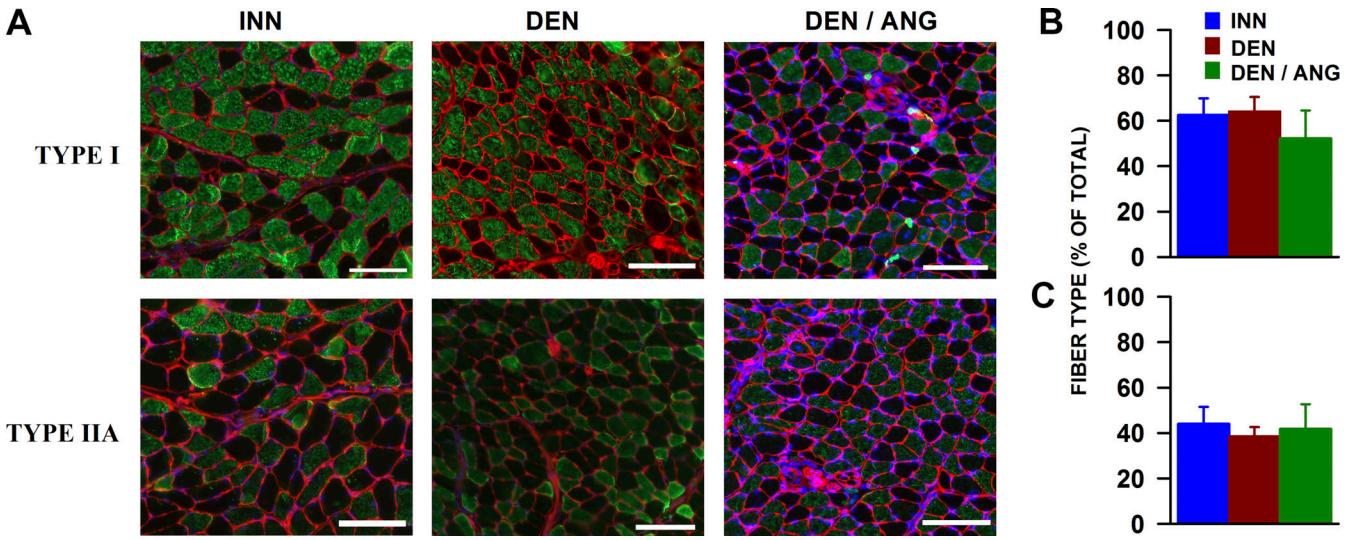

Figure 13. **Neither denervation nor Ang 1–7 affected the expression of myosin I and IIA in CD-1 soleus. (A)** Images of type I and IIA and fibers in innervated, denervated, and denervated Ang 1–7–treated EDL (DEN_ANG 1–7). **(B and C)** The number of fibers expressing myosin I (B) and myosin IIA (C) expressed as a percentage of the total number of fibers. Percent values were calculated for each muscle, and then mean and SE (vertical bars) were calculated from four or five muscles. Scale bars, 100 µm. The total number of fibers analyzed for innervated, denervated, and DEN-Ang 1–7 were 2,889, 2,877, and 3,826, respectively.

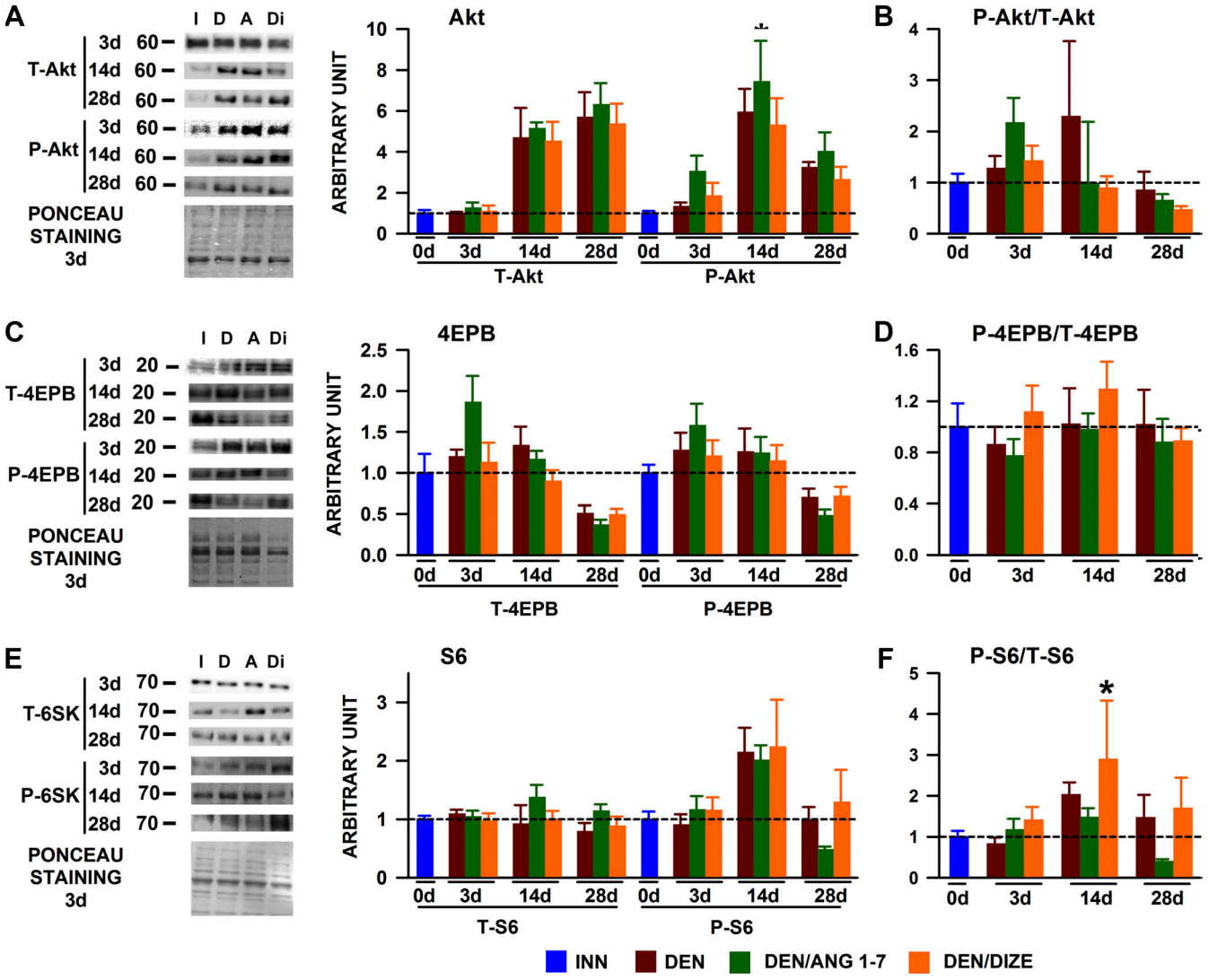

Figure 14. **In CD-1 EDL, Ang 1–7 did not significantly affect the changes in total (T) and phosphorylated Akt, 4EPB, and S6 protein content associated with 3, 14, and 28 d of denervation.** Protein content of total and phosphorylated (A) Akt, (C) 4EPB, (E) S6, phosphorylated/total ratio for (B) Akt, (D) 4EPB, and (F) S6 associated with 3, 14, and 28 d of denervation. Protein content was first normalized to the total protein content and then expressed relative to the content in innervated muscle. Ponceau staining is from the 3-d Western blots to provide an example for total proteins. A, denervated Ang 1–7 treated; D and DEN, denervated; Di, denervated-DIZE treated; I, INN, and 0 d, innervated; P, phosphorylated; T, total. Vertical bars represent the SE of six to eight muscles. *, Mean protein content significantly different from that of innervated muscle (ANOVA and LSD, $P < 0.05$).

potential overshoot and maximum rate of depolarization, which have been used as an index of Na^+ current during the depolarization phase (Hodgkin and Katz, 1949), were both depressed in denervated muscle fibers. Ang 1–7 and DIZE allowed for normal action potential overshoot in denervated muscle fibers despite small increases in maximum rate of depolarization. Thus, we suggest that the primary mechanism by which Ang 1–7 prevents the loss of normalized tetanic force is by preventing the membrane depolarization associated with denervation, allowing fibers to remain fully excitable with normal action potential amplitude.

It is interesting to note that changes in resting E_M during denervation with and without Ang 1–7 treatment occur to the same extent in denervated EDL and soleus despite the fact that the Na^+ K^+ pump content increases in the former muscle and decreases in the latter. Using the ^{3}H-ouabain–binding technique, 15- and 31-d denervation periods result in pump content that decreases by ∼35% in rat soleus and only 15% in rat EDL (Clausen et al., 1982; Ward et al., 1987). Thus, the decrease in soleus α1 and α2 pump content observed in this study is in agreement with previous studies, whereas the increase in EDL is not. The increase in pump content in mouse EDL may reflect a difference in species and may also be related to the large increase in the number of denervated fibers expressing type IIA fibers. Normal and innervated soleus muscle has fibers that primarily express type I (63%) and type IIA (51%) myosin (compared with only 2% and 16%, respectively, in normal and innervated EDL; this study). Furthermore, the higher number of type IIA in normal soleus is associated with a pump content that is two times greater than in normal EDL (Clausen et al.,

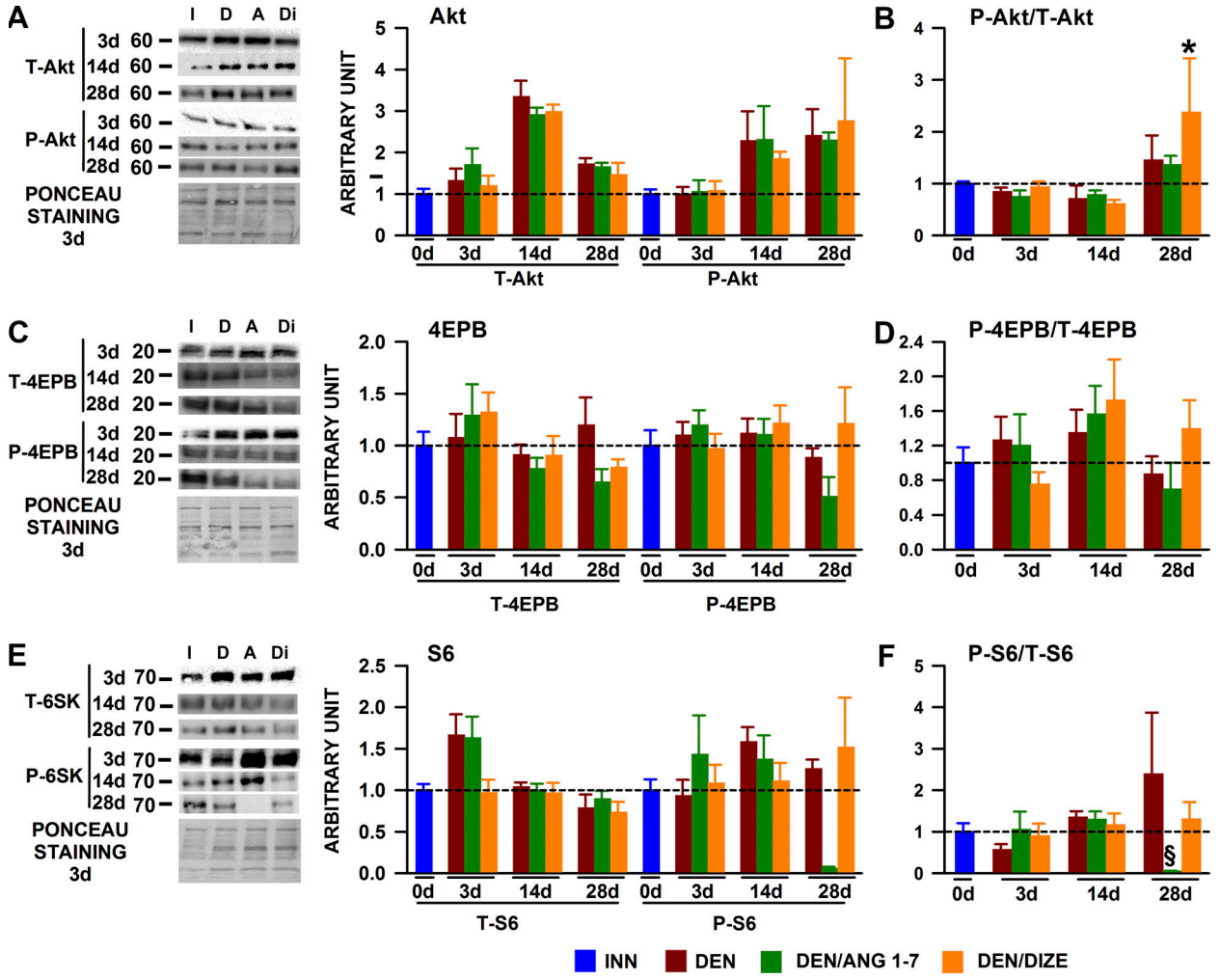

Figure 15. **In CD-1 soleus, Ang 1–7 mostly did not significantly affect the changes total and phosphorylated Akt, 4EPB, and S6 protein content associated with 3, 14, and 28 d of denervation.** Protein content of total and phosphorylated (A) Akt, (C) 4EPB, and (E) S6, and phosphorylated/total ratio for (B) Akt, (D) 4EPB, and (F) S6 associated with 3, 14, and 28 d of denervation. Protein contents were first normalized to the total protein content and then expressed relative to the content in innervated muscle. Ponceau staining is from the 3-d Western blots to provide an example for total proteins. Vertical bars represent the SE of six to eight muscles. *, Mean protein content significantly different from that of INN muscles; §, mean protein content significantly different from DEN muscles (ANOVA and LSD, $P < 0.05$).

2011; Ammar et al., 2015). Finally, in a hyperkalemic periodic paralysis (HyperKPP) mouse model, the number of EDL fibers that express type IIA myosin is ∼60% (Khogali et al., 2015) compared with 16% in normal EDL muscle (this study); again, the greater number of type IIA fibers in HyperKPP EDL is associated with a pump content that is two times greater than in normal EDL (Clausen et al., 2011; Ammar et al., 2015). Together, these facts suggest that fibers expressing type IIA myosin contain more Na^+ K^+ pump than fibers expressing type IIB myosin, and as the number of fibers expressing type IIA myosin increases to 95% in denervated EDL, there is a concomitant increase in pump content.

The next question is why the depolarization in denervated EDL and soleus muscles is the same with opposite changes in pump content and similar effects of Ang 1–7 on membrane excitability, despite the fact that Ang 1–7 increases the pump content only in EDL. Compared with normal muscles, HyperKPP EDL muscle fibers are largely depolarized and contain two times more Na^+ K^+ pump than normal muscles, with no increase in the pump electrogenic contribution. HyperKPP diaphragm, on the other hand, has similar resting E_M compared with normal diaphragm, because the pump electrogenic contribution is twice that in normal diaphragm, despite the fact that the pump content is not elevated (Ammar et al., 2015). It therefore appears that changes or the lack of pump content in both HyperKPP and denervated muscles cannot be an indication of the pump electrogenic contribution to the resting E_M. Thus, future studies will be necessary to fully understand how Ang 1–7 prevents membrane depolarization in denervated muscles by determining not only the pump electrogenic contribution but also whether Ang 1–7 reverses the increase in Na^+ permeability and decrease in K^+ permeability (Kotsias and Venosa, 1987), as well as changes in K^+ and Cl^- conductance, as all these components are known to affect resting E_M.

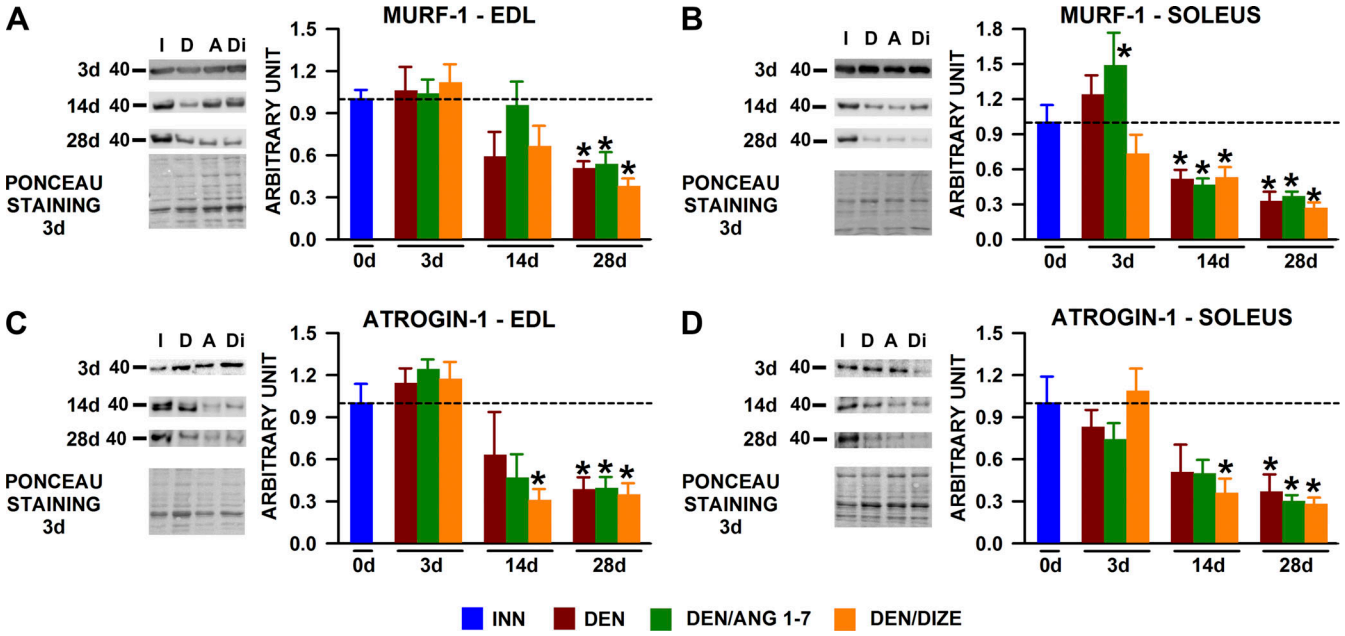

Figure 16. **In CD-1 EDL and soleus, Ang 1–7 had no significant effect on the changes MuRF-1 and atrogin-1 protein content associated with 3, 14, and 28 d of denervation.** Protein content of MURF-1 in (A) EDL and (B) soleus, and of atrogin-1 in (C) EDL and (D) soleus. Protein content was first normalized to the total protein content and then expressed relative to the content in innervated muscle. Ponceau staining is from the 3-d Western blots to provide an example for total proteins. Vertical bars represent the SE of six to eight muscles. *, Mean protein content significantly different from that of innervated muscles (ANOVA and LSD, $P < 0.05$).

Twitch force and force–frequency relationship

It is interesting that despite a decrease in action potential overshoot and a 60% loss in excitability, the normalized twitch force to CSA becomes greater in denervated EDL and soleus as previously reported (Finol et al., 1981; Dufresne et al., 2016). The decrease in mean overshoot to 1–5 mV is not expected to cause large decrease in twitch force, because twitch force decreases by ∼10% as overshoot decreases from 30 mV to 1–5 mV (Yensen et al., 2002; Cairns et al., 2003). One factor that may counteract the expected decrease in twitch force from the excitability loss is a prolongation of the twitch contraction (this study; Finol et al., 1981). Both time to peak and the relaxation phase are prolonged in denervated muscles, allowing more time to develop force during a twitch; whether other factors can also contribute to the increase in twitch force cannot be determined from this study. The further increases in twitch force by Ang 1–7–treated muscles can then be explained by the maintenance of membrane excitability as explained above.

The prolongation of the twitch contraction is also responsible for the major shift in the force–frequency relationship toward lower frequencies in both denervated EDL and soleus, because twitch contractions start to fuse at lower frequencies. Two causes of the twitch prolongation and shift in force–frequency relationship can be proposed: (1) a shift in the fiber type composition and (2) a decreased capacity of the Ca^{2+} ATPase pump to transport Ca^{2+} back in the sarcoplasmic reticulum. The maximum unloaded shortening velocity of type IIA single fibers is ∼23–35% slower than for type IIB for rat muscles; in mouse muscles, that difference is even greater, being 50% (Bottinelli et al., 1991; Bottinelli et al., 1994; Pellegrino et al., 2003). An increase in the number of type IIA fibers in denervated EDL, which have slower shortening velocities, would be expected to result in slower force development and thus lower twitch force. Furthermore, Ang 1–7 treatment further increases twitch force despite a reduction in the number of type IIA fibers. Finally, there was no change in fiber type composition in denervated soleus. It is therefore unlikely that greater twitch force in denervated fibers is due to a change in fiber type composition following denervation.

In EDL, the fast Ca^{2+} ATPase pump SERCA1 protein content decreases while that of the slow SERCA2 increases. More importantly, there is a net decrease in the maximal rate of the total Ca^{2+} ATPase activity; a decrease in the maximal rate also occurred in soleus, but to a smaller extent when compared with EDL (Dufresne et al., 2016). Such decreases in Ca^{2+} ATPase pump activity then slow down Ca^{2+} reuptake by the sarcoplasmic reticulum, resulting in prolonged increase in $[Ca^{2+}]_i$ and allowing more time to generate greater force during twitches. Finally, the lack of an Ang 1–7 effect on those two contractile parameters suggests that Ang 1–7 does not affect the denervation effect on the expression and activity of either SERCA1 or SERCA2.

Ang 1–7 has little effect on the atrophy and hypertrophy pathways

All Ang 1–7 effects on twitch and tetanic force were blocked by A779, a MasR antagonist, or absent in $MasR^{-/-}$ muscles (twitch force). A779 treatment also exacerbated the decrease in soleus fiber CSA during denervation. These results are in agreement with the fact that Ang 1–7 acts via its MasR in skeletal muscle. Interestingly, while the normalized tetanic forces of wild-type

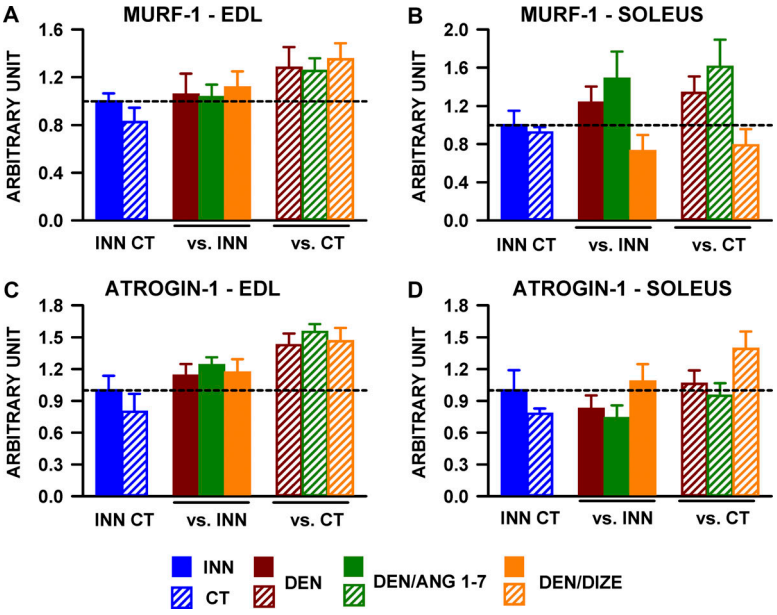

Figure 17. **Calculating changes in MuRF-1 and atrogin-1 protein content in denervated muscles using contralateral innervated muscle results in an overestimation.** Protein content of MURF-1 in (A) EDL and (B) soleus, and of atrogin-1 in (C) EDL and (D) soleus. MuRF-1 and atrogin-1 were measured in muscles from nondenervated mice (INN) and the innervated contralateral muscles of a denervated mice (CT). Changes in protein content for denervated, Ang 1–7– and DIZE-treated denervated muscles were then calculated relative to the data from INN or CT. The CT data are relative to INN data.

denervated EDL and soleus were respectively 35% and 56% less than those of their innervated counterparts, denervated MasR$^{-/-}$ soleus muscle develops a normalized tetanic force similar to that of the innervated soleus, whereas a 17% decrease was observed in MasR$^{-/-}$ EDL. The resting E_M depolarization in denervated MasR$^{-/-}$ was smaller than in denervated wild-type muscles, resulting in smaller but still significant decrease in membrane excitability. Furthermore, the overshoot was completely abolished in denervated MasR$^{-/-}$ muscles, as the action potential peak remained negative. Together these results suggest that the normalized tetanic force should be less in denervated than innervated MasR$^{-/-}$ muscles. There is therefore at least one other mechanism that prevents the decrease in normalized force, and future studies are necessary to elucidate this mechanism.

Denervation has a strong impact on the content and phosphorylation of the Akt–mTOR hypertrophic pathway. In regard to Akt, we observed no change in protein content after a 3-d denervation period but very large increases in both total and phosphorylated Akt after 14 and 28 d of denervation in EDL and after 14 d in soleus. Large increases in phosphorylated S6, a mTOR downstream target, was also observed after 14 d in EDL, while no change was observed for 4EPB, another mTOR target. It is surprising that the Akt–mTOR pathway (especially Akt) is activated after 14 and 28 d in EDL, a time when atrophy is expected to be high. However, the effect of denervation on total and phosphorylated Akt, S6, and 4EPB are in agreement with results recently published for the tibialis anterior muscle (MacDonald et al., 2014; Castets et al., 2019). Castets et al. actually suggested that a tight regulation of the Akt–mTOR pathway is required to maintain muscle homeostasis; a reduced activation promotes more atrophy, while a large and sustained activation of mTOR results in muscle myopathy, including formation of vacuoles, aggregates, and abnormal nuclei. Large decreases in MuRF-1 and atrogin-1 protein content were observed by 14 and 28 d, which is also in agreement with a large decrease in atrogin-1 after a 21-d denervation period (MacDonald et al., 2014). Considering the activation of the Akt pathway, which is known to inhibit the expression of both MuRF-1 and atrogin-1, and the conclusion of Castets et al. (2019), our results are not surprising; that is, the large decreases at 14 and 28 d are most likely because of inhibition from the Akt pathway.

It was, however, surprising that the 3-d denervation period resulted in small changes for MuRF-1 and atrogin-1 protein content; that is, there were 6% and 24% increases in MuRF-1 protein content for EDL and soleus, respectively while for atrogin-1, there was a 14% increase in EDL and a 17% decrease in soleus. These values are quite low compared with the 5- to 40-fold increase in MuRF-1 and atrogin-1 mRNA transcripts after a 3-d denervation period before returning to normal levels by day 14 (Sacheck et al., 2007; Macpherson et al., 2011; Milan et al., 2015). Compared with the increase in mRNA transcripts, the increases in MuRF-1 and atrogin-1 protein content are much smaller, being 1.3- to 5-fold after 6–7 d of denervation (Fjällström et al., 2014; Baumann et al., 2016; Guo et al., 2016; Lala-Tabbert et al., 2019; You et al., 2021). There is even one study reporting 20–30% decreases in MuRF-1 and atrogin-1 protein content in EDL and soleus after 4 d of denervation (Gao and Li, 2018). Although the antibody used in this study has also been used in many other studies, a shortcoming of the present work is that the MuRF-1 antibody specificity has not been verified using MuRF-1$^{-/-}$ skeletal muscle lysate. We must also take into account that in most studies, one leg is denervated while muscles from the contralateral leg are used as control innervated muscles, whereas in this study, our control innervated muscles were from mice that were not denervated. Denervating one leg results in an increased load to the contralateral leg, an effect that triggers hypertrophy. Notably, we found that MuRF-1 and atrogin-1 protein content of contralateral innervated EDL from denervated mice were 17% to 20% less than the content from normal innervated EDL from nondenervated mice (Fig. 17). If we now calculate the change in protein content between contralateral innervated and denervated muscles as in other studies, then

after 3-d denervation, MuRF-1 and atrogin-1 protein content increases by 28% and 43% in EDL, respectively. Similar calculations for soleus result in increases of 34% and 6%, respectively. Thus, one must be careful in using contralateral muscles, as it overestimates the changes in MuRF-1 and atrogin-1 protein content, and our results are perhaps a better representation of the changes in these proteins in EDL and soleus, at least for a 3-d denervation period.

Activation of MasR by Ang 1–7 is known to activate the Akt–mTOR pathway (Cisternas et al., 2015). However, Ang 1–7 and DIZE either has little effect or did not cause consistent increases or decreases on Akt, S6, and 4EPB, as well as for MuRF-1 and atrogin-1 protein content. We therefore suggest that the lack of an effect of Ang 1–7 on protein content detected during denervation is the reason why Ang 1–7 has no major effect on actin and myosin protein content, muscle mass, and fiber CSA. What remains to be determined is how Ang 1–7 improves membrane excitability and resting E_M in denervated muscles. However, as discussed above, future studies are first necessary to determine how Ang 1–7 modifies the activity of membrane components involved in resting E_M regulation and then determine whether the Akt pathway or another pathway is involved.

In conclusion, this study provides evidence that Ang 1–7 is very effective at preventing excessive force loss, as it maintains the normalized tetanic force to CSA to a level similar to that of innervated muscles, at least up to 28 d of denervation. A pharmacological approach using DIZE to increase Ang 1–7 levels is also as effective. The major mechanism for the maintenance of normalized tetanic force is likely to involve a reduction by Ang 1–7 treatment in the extent of the membrane depolarization associated with denervation, allowing for the maintenance of membrane excitability and normal action potential overshoot. Ang 1–7 was, on the other hand, ineffective at preventing muscle mass loss and fiber CSA reduction, possibly because it does not alter the level of Akt–mTOR activity or MuRF-1 and atrogin-1 protein content.

Acknowledgments

Henk L. Granzier served as editor.

Mohamed Thabet maintained the $MasR^{-/-}$ mouse colony and carried out genotyping.

This study was supported by a grant from the National Sciences and Engineering Research Council of Canada (#153604) and the Canadian Institutes of Health Research (#147314) to J.-M. Renaud. H.M. Albadrani had a scholarship from the Majmaah University, Kingdom of Saudi Arabia (represented by the Saudi Cultural Bureau, Canada).

The authors declare no competing financial interests.

Author contributions: H. Albadrani designed the study, carried out experiments and analyses, and wrote the manuscript. T. Ammar carried out experiments and analyses, and revised the manuscript. M. Bader generated the MasR knockout mouse model, and revised and approved the manuscript. J.-M. Renaud designed the study, carried out the statistical analyses, and revised and approved the manuscript.

Submitted: 19 December 2019
Revised: 30 June 2021
Accepted: 11 August 2021

References

Ábrigo, J., F. Simon, D. Cabrera, and C. Cabello-Verrugio. 2016. Angiotensin-(1-7) Prevents Skeletal Muscle Atrophy Induced by Transforming Growth Factor Type Beta (TGF-β) via Mas Receptor Activation. *Cell. Physiol. Biochem.* 40:27–38. https://doi.org/10.1159/000452522

Acuña, M.J., P. Pessina, H. Olguin, D. Cabrera, C.P. Vio, M. Bader, P. Muñoz-Canoves, R.A. Santos, C. Cabello-Verrugio, and E. Brandan. 2014. Restoration of muscle strength in dystrophic muscle by angiotensin-1-7 through inhibition of TGF-β signalling. *Hum. Mol. Genet.* 23:1237–1249. https://doi.org/10.1093/hmg/ddt514

Al-Amood, W.S., H.J. Finol, and D.M. Lewis. 1986. Chronic stimulation modifies the isotonic shortening velocity of denervated rat slow-twitch muscle. *Proc. R. Soc. Lond. B Biol. Sci.* 228:43–58. https://doi.org/10.1098/rspb.1986.0039

Albuquerque, E.X., and S. Thesleff. 1968. A comparative study of membrane properties of innervated and chronically denervated fast and slow skeletal muscles of the rat. *Acta Physiol. Scand.* 73:471–480. https://doi.org/10.1111/j.1365-201X.1968.tb10886.x

Albuquerque, E.X., F.T. Schuh, and F.C. Kauffman. 1971. Early membrane depolarization of the fast mammalian muscle after denervation. *Pflugers Arch.* 328:36–50. https://doi.org/10.1007/BF00587359

Ammar, T., W. Lin, A. Higgins, L.J. Hayward, and J.M. Renaud. 2015. Understanding the physiology of the asymptomatic diaphragm of the M1592V hyperkalemic periodic paralysis mouse. *J. Gen. Physiol.* 146:509–525. https://doi.org/10.1085/jgp.201511476

Baumann, C.W., H.M. Liu, and L.V. Thompson. 2016. Denervation-Induced Activation of the Ubiquitin-Proteasome System Reduces Skeletal Muscle Quantity Not Quality. *PLoS One.* 11:e0160839. https://doi.org/10.1371/journal.pone.0160839

Bottinelli, R., S. Schiaffino, and C. Reggiani. 1991. Force-velocity relations and myosin heavy chain isoform compositions of skinned fibres from rat skeletal muscle. *J. Physiol.* 437:655–672. https://doi.org/10.1113/jphysiol.1991.sp018617

Bottinelli, R., R. Betto, S. Schiaffino, and C. Reggiani. 1994. Maximum shortening velocity and coexistence of myosin heavy chain isoforms in single skinned fast fibres of rat skeletal muscle. *J. Muscle Res. Cell Motil.* 15:413–419. https://doi.org/10.1007/BF00122115

Cairns, S.P., J.A. Flatman, and T. Clausen. 1995. Relation between extracellular [K+], membrane potential and contraction in rat soleus muscle: modulation by the Na+-K+ pump. *Pflugers Arch.* 430:909–915. https://doi.org/10.1007/BF01837404

Cairns, S.P., W.A. Hing, J.R. Slack, R.G. Mills, and D.S. Loiselle. 1997. Different effects of raised [K+]o on membrane potential and contraction in mouse fast- and slow-twitch muscle. *Am. J. Physiol.* 273:C598–C611. https://doi.org/10.1152/ajpcell.1997.273.2.C598

Cairns, S.P., S.J. Buller, D.S. Loiselle, and J.M. Renaud. 2003. Changes of action potentials and force at lowered [Na+]o in mouse skeletal muscle: implications for fatigue. *Am. J. Physiol. Cell Physiol.* 285:C1131–C1141. https://doi.org/10.1152/ajpcell.00401.2002

Castets, P., N. Rion, M. Théodore, D. Falcetta, S. Lin, M. Reischl, F. Wild, L. Guérard, C. Eickhorst, M. Brockhoff, et al. 2019. mTORC1 and PKB/Akt control the muscle response to denervation by regulating autophagy and HDAC4. *Nat. Commun.* 10:3187. https://doi.org/10.1038/s41467-019-11227-4

Chibalin, A.V., J.A. Heiny, B. Benziane, A.V. Prokofiev, A.V. Vasiliev, V.V. Kravtsova, and I.I. Krivoi. 2012. Chronic nicotine modifies skeletal muscle Na,K-ATPase activity through its interaction with the nicotinic acetylcholine receptor and phospholemman. *PLoS One.* 7:e33719. https://doi.org/10.1371/journal.pone.0033719

Cisternas, F., M.G. Morales, C. Meneses, F. Simon, E. Brandan, J. Abrigo, Y. Vazquez, and C. Cabello-Verrugio. 2015. Angiotensin-(1-7) decreases skeletal muscle atrophy induced by angiotensin II through a Mas receptor-dependent mechanism. *Clin. Sci. (Lond.).* 128:307–319. https://doi.org/10.1042/CS20140215

Clausen, T., L.C. Sellin, and S. Thesleff. 1981. Quantitative changes in ouabain binding after denervation and during reinnervation of mouse skeletal muscle. *Acta Physiol. Scand.* 111:373–375. https://doi.org/10.1111/j.1748-1716.1981.tb06750.x

Clausen, T., O. Hansen, K. Kjeldsen, and A. Nørgaard. 1982. Effect of age, potassium depletion and denervation on specific displaceable [3H] ouabain binding in rat skeletal muscle in vivo. *J. Physiol.* 333:367–381. https://doi.org/10.1113/jphysiol.1982.sp014458

Clausen, T., O.B. Nielsen, J.D. Clausen, T.H. Pedersen, and L.J. Hayward. 2011. Na^+,K^+-pump stimulation improves contractility in isolated muscles of mice with hyperkalemic periodic paralysis. *J. Gen. Physiol.* 138:117–130. https://doi.org/10.1085/jgp.201010586

de Moraes, P.L., L.M. Kangussu, C.H. Castro, A.P. Almeida, R.A.S. Santos, and A.J. Ferreira. 2017. Vasodilator Effect of Angiotensin-(1-7) on Vascular Coronary Bed of Rats: Role of Mas, ACE and ACE2. *Protein Pept. Lett.* 24: 869–875. https://doi.org/10.2174/0929866524666170728154459

Dufresne, S.S., N.A. Dumont, A. Boulanger-Piette, V.A. Fajardo, D. Gamu, S.A. Kake-Guena, R.O. David, P. Bouchard, É. Lavergne, J.M. Penninger, et al. 2016. Muscle RANK is a key regulator of Ca2+ storage, SERCA activity, and function of fast-twitch skeletal muscles. *Am. J. Physiol. Cell Physiol.* 310:C663–C672. https://doi.org/10.1152/ajpcell.00285.2015

Echeverría-Rodríguez, O., L. Del Valle-Mondragón, and E. Hong. 2014. Angiotensin 1-7 improves insulin sensitivity by increasing skeletal muscle glucose uptake in vivo. *Peptides.* 51:26–30. https://doi.org/10.1016/j.peptides.2013.10.022

Edwards, J.N., W.A. Macdonald, C. van der Poel, and D.G. Stephenson. 2007. O2(*-) production at 37 ° C plays a critical role in depressing tetanic force of isolated rat and mouse skeletal muscle. *Am. J. Physiol. Cell Physiol.* 293:C650–C660. https://doi.org/10.1152/ajpcell.00037.2007

Fernandes, T., N.Y. Hashimoto, and E.M. Oliveira. 2010. Characterization of angiotensin-converting enzymes 1 and 2 in the soleus and plantaris muscles of rats. *Braz. J. Med. Biol. Res.* 43:837–842. https://doi.org/10.1590/S0100-879X2010007500088

Finol, H.J., D.M. Lewis, and R. Owens. 1981. The effects of denervation on contractile properties or rat skeletal muscle. *J. Physiol.* 319:81–92. https://doi.org/10.1113/jphysiol.1981.sp013893

Fjällström, A.K., K. Evertsson, M. Norrby, and S. Tågerud. 2014. Forkhead box O1 and muscle RING finger 1 protein expression in atrophic and hypertrophic denervated mouse skeletal muscle. *J. Mol. Signal.* 9:9. https://doi.org/10.1186/1750-2187-9-9

Fu, Z., L. Zhao, K.W. Aylor, R.M. Carey, E.J. Barrett, and Z. Liu. 2014. Angiotensin-(1-7) recruits muscle microvasculature and enhances insulin's metabolic action via mas receptor. *Hypertension.* 63:1219–1227. https://doi.org/10.1161/HYPERTENSIONAHA.113.03025

Gao, H., and Y.F. Li. 2018. Distinct signal transductions in fast- and slow-twitch muscles upon denervation. *Physiol. Rep.* 6:e13606. https://doi.org/10.14814/phy2.13606

Guo, Y., J. Meng, Y. Tang, T. Wang, B. Wei, R. Feng, B. Gong, H. Wang, G. Ji, and Z. Lu. 2016. AMP-activated kinase α2 deficiency protects mice from denervation-induced skeletal muscle atrophy. *Arch. Biochem. Biophys.* 600:56–60. https://doi.org/10.1016/j.abb.2016.04.015

Hinkle, R.T., K.M.B. Hodge, D.B. Cody, R.J. Sheldon, B.K. Kobilka, and R.J. Isfort. 2002. Skeletal muscle hypertrophy and anti-atrophy effects of clenbuterol are mediated by the beta2-adrenergic receptor. *Muscle Nerve.* 25:729–734. https://doi.org/10.1002/mus.10092

Hinkle, R.T., E. Dolan, D.B. Cody, M.B. Bauer, and R.J. Isfort. 2005. Phosphodiesterase 4 inhibition reduces skeletal muscle atrophy. *Muscle Nerve.* 32:775–781. https://doi.org/10.1002/mus.20416

Hodgkin, A.L., and B. Katz. 1949. The effect of sodium ions on the electrical activity of giant axon of the squid. *J. Physiol.* 108:37–77. https://doi.org/10.1113/jphysiol.1949.sp004310

Khogali, S., B. Lucas, T. Ammar, D. Dejong, M. Barbalinardo, L.J. Hayward, and J.M. Renaud. 2015. Physiological basis for muscle stiffness and weakness in a knock-in M1592V mouse model of hyperkalemic periodic paralysis. *Physiol. Rep.* 3:e12656. https://doi.org/10.14814/phy2.12656

Kotsias, B.A., and R.A. Venosa. 1987. Role of sodium and potassium permeabilities in the depolarization of denervated rat muscle fibres. *J. Physiol.* 392:301–313. https://doi.org/10.1113/jphysiol.1987.sp016781

Lala-Tabbert, N., R. Lejmi-Mrad, K. Timusk, M. Fukano, J. Holbrook, M. St-Jean, E.C. LaCasse, and R.G. Korneluk. 2019. Targeted ablation of the cellular inhibitor of apoptosis 1 (cIAP1) attenuates denervation-induced skeletal muscle atrophy. *Skelet. Muscle.* 9:13. https://doi.org/10.1186/s13395-019-0201-6

MacDonald, E.M., E. Andres-Mateos, R. Mejias, J.L. Simmers, R. Mi, J.S. Park, S. Ying, A. Hoke, S.J. Lee, and R.D. Cohn. 2014. Denervation atrophy is independent from Akt and mTOR activation and is not rescued by myostatin inhibition. *Dis. Model. Mech.* 7:471–481. https://doi.org/10.1242/dmm.014126

Macpherson, P.C., X. Wang, and D. Goldman. 2011. Myogenin regulates denervation-dependent muscle atrophy in mouse soleus muscle. *J. Cell. Biochem.* 112:2149–2159. https://doi.org/10.1002/jcb.23136

Marcus, Y., G. Shefer, K. Sasson, F. Kohen, R. Limor, O. Pappo, N. Nevo, I. Biton, M. Bach, T. Berkutzki, et al. 2013. Angiotensin 1-7 as means to prevent the metabolic syndrome: lessons from the fructose-fed rat model. *Diabetes.* 62:1121–1130. https://doi.org/10.2337/db12-0792

Martinez, P.F., K. Okoshi, L.A. Zornoff, R.F. Carvalho, S.A. Oliveira Junior, A.R. Lima, D.H. Campos, R.L. Damatto, C.R. Padovani, C.R. Nogueira, et al. 2010. Chronic heart failure-induced skeletal muscle atrophy, necrosis, and changes in myogenic regulatory factors. *Med. Sci. Monit.* 16: BR374–BR383.

Meneses, C., M.G. Morales, J. Abrigo, F. Simon, E. Brandan, and C. Cabello-Verrugio. 2015. The angiotensin-(1-7)/Mas axis reduces myonuclear apoptosis during recovery from angiotensin II-induced skeletal muscle atrophy in mice. *Pflugers Arch.* 467:1975–1984. https://doi.org/10.1007/s00424-014-1617-9

Milan, G., V. Romanello, F. Pescatore, A. Armani, J.H. Paik, L. Frasson, A. Seydel, J. Zhao, R. Abraham, A.L. Goldberg, et al. 2015. Regulation of autophagy and the ubiquitin-proteasome system by the FoxO transcriptional network during muscle atrophy. *Nat. Commun.* 6:6670. https://doi.org/10.1038/ncomms7670

Morales, M.G., J. Abrigo, C. Meneses, F. Cisternas, F. Simon, and C. Cabello-Verrugio. 2015a. Expression of the Mas receptor is upregulated in skeletal muscle wasting. *Histochem. Cell Biol.* 143:131–141. https://doi.org/10.1007/s00418-014-1275-1

Morales, M.G., H. Olguín, G. Di Capua, E. Brandan, F. Simon, and C. Cabello-Verrugio. 2015b. Endotoxin-induced skeletal muscle wasting is prevented by angiotensin-(1-7) through a p38 MAPK-dependent mechanism. *Clin. Sci. (Lond.).* 129:461–476. https://doi.org/10.1042/CS20140840

Morales, M.G., J. Abrigo, M.J. Acuña, R.A. Santos, M. Bader, E. Brandan, F. Simon, H. Olguin, D. Cabrera, and C. Cabello-Verrugio. 2016. Angiotensin-(1-7) attenuates disuse skeletal muscle atrophy in mice via its receptor, Mas. *Dis. Model. Mech.* 9:441–449. https://doi.org/10.1242/dmm.023390

Mori, J., V.B. Patel, T. Ramprasath, O.A. Alrob, J. DesAulniers, J.W. Scholey, G.D. Lopaschuk, and G.Y. Oudit. 2014. Angiotensin 1-7 mediates renoprotection against diabetic nephropathy by reducing oxidative stress, inflammation, and lipotoxicity. *Am. J. Physiol. Renal Physiol.* 306:F812–F821. https://doi.org/10.1152/ajprenal.00655.2013

Murphy, K.T., M.I. Hossain, K. Swiderski, A. Chee, T. Naim, J. Trieu, V. Haynes, S.J. Read, D.I. Stapleton, S.M. Judge, et al. 2019. Mas Receptor Activation Slows Tumor Growth and Attenuates Muscle Wasting in Cancer. *Cancer Res.* 79:706–719. https://doi.org/10.1158/0008-5472.CAN-18-1207

Oh, Y.B., J.H. Kim, B.M. Park, B.H. Park, and S.H. Kim. 2012. Captopril intake decreases body weight gain via angiotensin-(1-7). *Peptides.* 37:79–85. https://doi.org/10.1016/j.peptides.2012.06.005

Pellegrino, C., and C. Franzini. 1963. An Electron Microscope Study of Denervation Atrophy in Red and White Skeletal Muscle Fibers. *J. Cell Biol.* 17:327–349. https://doi.org/10.1083/jcb.17.2.327

Pellegrino, M.A., M. Canepari, R. Rossi, G. D'Antona, C. Reggiani, and R. Bottinelli. 2003. Orthologous myosin isoforms and scaling of shortening velocity with body size in mouse, rat, rabbit and human muscles. *J. Physiol.* 546:677–689. https://doi.org/10.1113/jphysiol.2002.027375

Riquelme, C., M.J. Acuña, J. Torrejón, D. Rebolledo, D. Cabrera, R.A. Santos, and E. Brandan. 2014. ACE2 is augmented in dystrophic skeletal muscle and plays a role in decreasing associated fibrosis. *PLoS One.* 9:e93449. https://doi.org/10.1371/journal.pone.0093449

Sacheck, J.M., J.P. Hyatt, A. Raffaello, R.T. Jagoe, R.R. Roy, V.R. Edgerton, S.H. Lecker, and A.L. Goldberg. 2007. Rapid disuse and denervation atrophy involve transcriptional changes similar to those of muscle wasting during systemic diseases. *FASEB J.* 21:140–155. https://doi.org/10.1096/fj.06-6604com

Santos, R.A.S., W.O. Sampaio, A.C. Alzamora, D. Motta-Santos, N. Alenina, M. Bader, and M.J. Campagnole-Santos. 2018. The ACE2/Angiotensin-(1-7)/MAS Axis of the Renin-Angiotensin System: Focus on Angiotensin-(1-7). *Physiol. Rev.* 98:505–553. https://doi.org/10.1152/physrev.00023.2016

Shavlakadze, T., J.D. White, M. Davies, J.F. Hoh, and M.D. Grounds. 2005. Insulin-like growth factor I slows the rate of denervation induced skeletal muscle atrophy. *Neuromuscul. Disord.* 15:139–146. https://doi.org/10.1016/j.nmd.2004.10.013

Steel, R.G.D, and J.H. Torrie. 1980. Principles and Procedures of Statistics: A Biometrical Approach. McGraw-Hill Book Company, New York.

Vandenburgh, H.H., P. Karlisch, J. Shansky, and R. Feldstein. 1991. Insulin and IGF-I induce pronounced hypertrophy of skeletal myofibers in tissue culture. *Am. J. Physiol.* 260:C475–C484. https://doi.org/10.1152/ajpcell.1991.260.3.C475

Vyskocil, F., B. Carlson, and E. Gutmann. 1973. Changes in resting membrane potential and contractility of innervated and denervated skeletal muscle free grafts in the rat. *Pflugers Arch.* 344:181–186. https://doi.org/10.1007/BF00586551

Walther, T., D. Balschun, J.P. Voigt, H. Fink, W. Zuschratter, C. Birchmeier, D. Ganten, and M. Bader. 1998. Sustained long term potentiation and anxiety in mice lacking the Mas protooncogene. *J. Biol. Chem.* 273: 11867–11873. https://doi.org/10.1074/jbc.273.19.11867

Ward, K.M., W. Manning, and A.C. Wareham. 1987. Effects of denervation and immobilisation during development upon [3H]ouabain binding by slow- and fast-twitch muscle of the rat. *J. Neurol. Sci.* 78:213–224. https://doi.org/10.1016/0022-510X(87)90062-1

Wareham, A.C. 1978. Effect of denervation and ouabain on the response of the resting membrane potential of rat skeletal muscle to potassium. *Pflugers Arch.* 373:225–228. https://doi.org/10.1007/BF00580828

Xu, J., R. Li, B. Workeneh, Y. Dong, X. Wang, and Z. Hu. 2012. Transcription factor FoxO1, the dominant mediator of muscle wasting in chronic kidney disease, is inhibited by microRNA-486. *Kidney Int.* 82:401–411. https://doi.org/10.1038/ki.2012.84

Yang, X., P. Xue, H. Chen, M. Yuan, Y. Kang, D. Duscher, H.G. Machens, and Z. Chen. 2020. Denervation drives skeletal muscle atrophy and induces mitochondrial dysfunction, mitophagy and apoptosis via miR-142a-5p/MFN1 axis. *Theranostics*. 10:1415–1432. https://doi.org/10.7150/thno.40857

Yensen, C., W. Matar, and J.M. Renaud. 2002. K+-induced twitch potentiation is not due to longer action potential. *Am. J. Physiol. Cell Physiol.* 283: C169–C177. https://doi.org/10.1152/ajpcell.00549.2001

You, J.S., K. Kim, N.D. Steinert, J. Chen, and T.A. Hornberger. 2021. mTORC1 mediates fiber type-specific regulation of protein synthesis and muscle size during denervation. *Cell Death Discov.* 7:74. https://doi.org/10.1038/s41420-021-00460-w

Zeman, R.J., R. Ludemann, and J.D. Etlinger. 1987. Clenbuterol, a beta 2-agonist, retards atrophy in denervated muscles. *Am. J. Physiol.* 252: E152–E155. https://doi.org/10.1152/ajpendo.1987.252.1.E152

Zhang, Y., J. Liu, J.Y. Luo, X.Y. Tian, W.S. Cheang, J. Xu, C.W. Lau, L. Wang, W.T. Wong, C.M. Wong, et al. 2015. Upregulation of Angiotensin (1-7)-Mediated Signaling Preserves Endothelial Function Through Reducing Oxidative Stress in Diabetes. *Antioxid. Redox Signal.* 23:880–892. https://doi.org/10.1089/ars.2014.6070